

## **On the effect of prevalent carbazole homocoupling defects on the photovoltaic performance of PCDTBT:PC<sub>71</sub>BM solar cells**

*Florian Lombeck, Hartmut Komber, Daniele Fazzi, Diego Nava, Jochen Kuhlmann, Dominik Stegerer, Karen Strassel, Josef Brandt, Amaia Diaz de Zerio Mendaza, Christian Müller, Walter Thiel, Mario Caironi, Richard Friend, Michael Sommer\**

F. Lombeck, J. Kuhlmann, D. Stegerer, K. Strassel, Dr. M. Sommer  
Makromolekulare Chemie, Stefan-Meier-Str. 31, Universität Freiburg, 79104 Freiburg,  
Germany

E-mail: michael.sommer@makro.uni-freiburg.de

F. Lombeck, Prof. R. Friend

Optoelectronics Group, Cavendish Laboratory, University of Cambridge, J. J. Thomson  
Avenue, Cambridge CB3 0HE, U.K.

J. Brandt, Dr. H. Komber

Leibniz-Institut für Polymerforschung Dresden e.V., Hohe Straße 6, 01069 Dresden, Germany

Dr. D. Fazzi, Prof. Dr. W. Thiel

Max-Planck-Institut für Kohlenforschung, Kaiser-Wilhelm-Platz 1, D-45470 Mülheim an der  
Ruhr, Germany

D. Nava, Dr. M. Caironi

Center for Nano Science and Technology @PoliMi, Istituto Italiano di Tecnologia  
Via Pascoli 70/3, Milano 20133, Italy.

D. Nava

Politecnico di Milano, Dipartimento di Fisica, P.za L. da Vinci 32, Milano 20133, Italy

A. Diaz de Zerio Mendaza, Dr. C. Müller

Department of Chemistry and Chemical Engineering, Chalmers University of Technology,  
41296 Göteborg, Sweden

Dr. M. Sommer

Freiburger Materialforschungszentrum, Stefan-Meier-Str. 21, 79104, Freiburg

Freiburger Institut für interaktive Materialien und bioinspirierte Technologien, Georges-  
Köhler-Allee 105, Universität Freiburg, 79110 Freiburg, Germany

Keywords: solar cells, PCDTBT, conjugated polymers, homocoupling defects, Suzuki  
polycondensation

## Abstract

We investigate the photophysical properties and solar cell performance of the classical donor-acceptor copolymer poly(N-9'-heptadecanyl-2,7-carbazole-alt-5,5-(4',7'-di-2-thienyl-2',1',3'-benzothiadiazole)) (PCDTBT) in relation to unintentionally formed main chain defects.

Carbazole-carbazole homocouplings (Cbz hc) are found to significant extent in PCDTBT made with a variety of Suzuki polycondensation conditions. Cbz hc vary between 0- 8 mol.-% depending on the synthetic protocol used, and are quantified by detailed NMR spectroscopy including model compounds, which allows to establish a UV-vis calibration curve. The results are corroborated by extended (TD)DFT investigations on the structural, electronic and optical properties of regularly alternating and homocoupled chains. The photovoltaic properties of PCDTBT:PC<sub>71</sub>BM blend solar cells significantly depend on the Cbz hc content for constant molecular weight, whereby an increasing amount of Cbz hc leads to strongly decreased short circuit currents  $J_{SC}$ . With increasing Cbz hc content,  $J_{SC}$  decreases more strongly than the intensity of the low energy absorption band, suggesting that small losses in absorption cannot explain the decrease in  $J_{SC}$  alone, but from combined effects of a more localized LUMO level on the TBT unit and lower hole mobilities found in highly defective samples. Homocoupling-free PCDTBT with optimized molecular weight yields the highest efficiency up to 7.2 % without extensive optimization.

## 1. Introduction

Conjugated polymers are a class of extensively investigated  $\pi$ -conjugated materials suitable for a multitude of applications ranging from e.g. photovoltaics<sup>[1]</sup>, field-effect transistors<sup>[2]</sup>, light-emitting diodes<sup>[3]</sup> and memory devices<sup>[4]</sup> to sensors and thermoelectric generators.<sup>[5]</sup> Within the last decades, an overwhelmingly large number of different building blocks have been used to construct numerous conjugated polymers with pre-selected and fine-tuned optoelectronic properties.<sup>[6,7]</sup> However, while structural diversity of conjugated materials is continuously broadening, the synthetic methods employed are often very similar. In most cases, transition metal-catalyzed polycondensation techniques based on two symmetric monomers are used, which, in the ideal case, lead to strictly alternating sequences. Therefore, when drawing the repeat unit of a conjugated polymer on paper, an alternating structure is implicitly assumed. However, it is also known that besides typical cross-coupling products other products can form due to homocoupling (hc) reactions, depending on a variety of reaction parameters.<sup>[8-12]</sup> The reason this may be a decisive factor when synthesizing conjugated polymers for organic electronics is that small degrees of polymerization are often obtained and, hence, any deviation from an alternating chain structure constitutes a non-negligible fraction of the chain, which consequently exhibits altered optoelectronic properties. The most common possibility for main chain electronic defects arises from hc reactions as seen with Kumada<sup>[13]</sup>, Suzuki<sup>[14-16]</sup>, and direct arylation polycondensations.<sup>[17-20]</sup> For Stille polycondensations, homocoupling reactions have been claimed to be present as well.<sup>[21,22]</sup> If occurring during polycondensation, covalent incorporation into the conjugated polymer backbone takes place and the resulting defects cannot be removed subsequently. Homocoupling reactions in Suzuki small molecule<sup>[11]</sup> and polycondensation reactions are assumed to be caused by the coupling of polymer chains having boronic ester end groups as shown by early work of Heitz *et al.* and by us recently.<sup>[14,16]</sup> Interestingly, the impact of hc and thus main chain defects on the optoelectronic performance of conjugated materials

remains largely unknown. Hendriks *et al.* recently reported the detrimental effect of intentionally homocoupled dithienyl-diketopyrrolopyrrole (DPP) units in DPP copolymers on their solar cell performance. In this case, DPP-DPP hc were shown to be present on the basis of explicitly designed defect comonomers and UV-vis spectroscopy experiments.<sup>[15]</sup> On the basis of these results there is strong indication that hc defects may be present in many other systems as well. As quantification of homocouplings is challenging, both their extent as well as their effect on opto-electronic properties is largely unknown. Thus, the investigation of defect-function relationships appears to be crucially important for further improving device performance and to ensure comparability and reproducibility of device performance.

Here, we investigate the impact of carbazole-carbazole homocouplings (Cbz hc) present in the often used conjugated polymer PCDTBT on its solar cell performance in blend films with PC<sub>71</sub>M as acceptor material. Using PCDTBT:PC<sub>71</sub>M blends, power conversion efficiencies (PCE) up to ~7% and internal quantum efficiencies approaching 100% have been reported.<sup>[23–25]</sup> At the same time, a broad range of PCE values from 3.5% – 7% can be found in the literature.<sup>[25]</sup> PCDTBT additionally offers excellent stability and operational lifetime of photovoltaic devices.<sup>[26,27]</sup> Using model dimers and PCDTBT with intentionally introduced Cbz hc, we first identify the <sup>1</sup>H NMR chemical shifts of both TBT as well as Cbz hc sequences, and subsequently quantify their occurrence for a variety of different Suzuki polycondensation protocols. While we find Cbz hc to occur under almost every catalytic condition used, TBT homocouplings are seldom found, and, if at all, with very low intensity. From <sup>1</sup>H NMR and UV-vis spectroscopy a calibration curve is established from which the Cbz hc content can simply be determined. (TD)DFT calculations further support the experimental findings. Changes in the UV-Vis band intensities can be reproduced upon the insertion of hc defects, and effects of hc defects on intra-molecular hole reorganization energies are small. Finally we show that the photovoltaic performance of PCDTBT:PC<sub>71</sub>BM blends substantially deteriorates with increasing content of Cbz hc, which can partially be

ascribed to reduced absorption by the charge-transfer band, and eventually to a more localized LUMO level on the TBT unit. As PCDTBT synthesis reported in the literature is mostly performed under conditions leading to defective materials, this work provides an explanation why comparability of device data is generally challenging. For future studies main chain electronic defects in conjugated polymers arising from homocoupling reactions must be considered as an additional parameter next to molecular weight and dispersity.

## 2. Results and discussion

### 2.1. Synthesis and materials

All synthetic procedures are described in detail in the Supporting Information. The dimer models are abbreviated as Cbz-Cbz, TBT-TBT and Cbz-TBT; for chemical structures see Supporting Information. PCDTBT is prepared by varying Suzuki polycondensation (SPC) protocols and is numbered as PCDTBT **1-11**. Molecular weights are determined by high temperature size exclusion chromatography (HT-SEC) in 1,2,4-trichlorobenzene at 150°C and, to ensure compatibility with the majority of existing literature, given relative to polystyrene standards (**Table 1**). We used viscosity detection to extract the Mark-Houwink parameters  $K$  and  $\alpha$  and thus attempted to establish a universal calibration, and found that molecular weights obtained from universal calibration were too low when compared to qualitative values from  $^1\text{H}$  NMR (**Table S1**). Table 1 also collects all important information of the PCDTBT samples used. Typical synthesis procedures are denoted as conditions i)-v) and are described in **Scheme 1a** as well as in detail in the Supporting Information. Catalysts were selected according to their appearance in the literature, air stability and activity. Generally, it was found that the type of Pd precursor has the largest influence on the amount of Cbz homocouplings, with  $\text{Pd}(\text{PPh}_3)_4$  being the only catalyst that enabled the synthesis of homocoupling-free PCDTBT **1**, **7** and **11** with different molecular weight. All other catalytic systems, including  $\text{P}_2\text{dba}_3$ /phosphine, third generation Buchwald catalyst G3/ phosphine and

G2[*o*-tolyl<sub>3</sub>]<sup>[28]</sup> led to varying Cbz hc contents of 2- 8 mol-% (PCDTBT **2-5, 8, 9**). Model copolymers PCDTBT **6** and **10** with intentionally introduced carbazole homocoupling defects were made by incorporating 10 mol-% of an asymmetric carbazole comonomer leading to Cbz dimer sequences (Scheme 1b). Importantly, as molecular weight affects photovoltaic performance of PCDTBT:PC<sub>71</sub>BM blends as well<sup>[29]</sup>, two series of PCDTBT with similar weight average molecular weights of  $M_w \sim 30$  kDa and 60 kDa, obtained as chloroform and chlorobenzene fractions, respectively, but varying defect concentration were selected for further analysis (Table 1). We prefer to use  $M_w$  rather than  $M_n$  values for comparison as the latter ones are much more sensitive to small variations in oligomer intensity. Usage of different molecular weight is highly important to elucidate effects of varying chain lengths. This is important especially for conjugated polymers where the degrees of polymerization are generally low. Thus, PCDTBT **1-6** with a similar  $M_w$  of 30 kDa and PCDTBT **7-10** with similar  $M_w$  of 60 kDa were used for the investigation of defect-function relationships.

## 2.2. Identification and quantification of Cbz and TBT homocouplings

Recently, we have shown Cbz hc to occur during the synthesis of PCDTBT and hexyl-substituted PCDTBT derivatives by direct arylation polycondensation and SPC.<sup>[16,17]</sup> Here, we quantify the signals of Cbz hc in PCDTBT in relation to a variety of SPC conditions. Additionally, we also elucidated whether TBT homocouplings formed with measurable content. To this end, we used the <sup>1</sup>H NMR data of the dimer TBT-TBT to estimate the chemical shifts of TBT hc in a Cbz-TBT-TBT-Cbz sequence taking into account chemical shift effects of neighboring Cbz units (for a detailed analysis see Supporting Information). The thiophene protons of the central T-T unit showed up as doublets with a coupling constant of  $\sim 3.2$  Hz at  $\sim 7.44$  and  $\sim 8.16$  ppm. Thus, for the identification of possible TBT-TBT sequences in PCDTBT, the 7.44 ppm signal appeared ideal, as overlap with backbone signals is not present (**Figure SI-2**). Unfortunately, protonated carbazole end groups (Cbz-H) arising

from protio-deborylation resulted in a triplet at this same position with a coupling constant of 7.5 Hz.<sup>[17]</sup> In principle, the two different coupling constants allowed to distinguish between TBT hc and Cbz-H end groups. Careful inspection of all PCDTBT spectra unequivocally proved the presence of TBT hc only for PCDTBT **8** as confirmed also by correlation peaks between signals at 7.47 ppm and 8.18 ppm in its TOCSY spectrum (see **Figure SI 3**).

However, the TBT hc content of PCDTBT **8** was very low and hence could not reliably be quantified. While TBT hc cannot be entirely ruled out for other samples, but could, compared to the frequently and much more intensely occurring Cbz hc, be clearly neglected. Therefore, in the present study we focus on how changes in the opto-electronic properties of PCDTBT evolve for Cbz hc contents of 0-10 mol-%. In order to assign the Cbz hc unit unambiguously, the <sup>1</sup>H chemical shifts were estimated by the aforementioned model approach based on dimers Cbz-Cbz and Cbz-TBT (see Supporting Information). To confirm these estimations, model PCDTBT **6** and **10** with intentionally introduced isolated Cbz dimer sequences mimicking the Cbz hc were prepared (Scheme 1b). Estimated and experimental <sup>1</sup>H chemical shift values were in very good agreement. Two characteristic doublets at 8.16 ppm and 8.23 ppm allowed quantifying the Cbz hc content, whereas the remaining four signals were overlapped by backbone signals. Similarly to the definition of regioregularity of P3HT,<sup>[13]</sup> we defined the Cbz hc content as the amount of Cbz-Cbz *linkages* divided by the total number of both Cbz-Cbz and Cbz-TBT *linkages*. It is reasonable to assume that the monomer feed content of 10 mol-% of the asymmetric Cbz comonomer was fully incorporated into PCDTBT **6** and **10** (Scheme 1b, Table 1). Deconvolution of the 8.35 – 8.1 ppm region results in signal intensities for Cbz-Cbz and Cbz-TBT linkages, and indeed a Cbz hc content of 10 mol-% was found for PCDTBT **10** and **11** (see SI). As for these two entries a catalytic system giving 2-3 % unintentional Cbz hc was used, a Cbz hc value of 12-13 % could have been expected. However, this is not confirmed by <sup>1</sup>H NMR and might be explained by the fact that microwave heating was used, in which cases generally lower homocoupling contents were

found. All other PCDTBT samples made under varying Suzuki conditions (Scheme 1a) were inspected with respect to Cbz hc and, if present, the Cbz hc content was determined by deconvolution or by comparison to deconvoluted samples (Table 1). The accuracy of both approaches depends on the line width and the content of TBT-H end groups, which also give signals in the 8.35 – 8.1 ppm region. As an example, **Figure 1** shows high temperature  $^1\text{H}$  NMR spectra of the two PCDTBT samples **6** and **7** with high molecular weight. PCDTBT **6** was made with intentionally introduced 10 mol-% Cbz hc, while PCDTBT **7** (Figure 1b) is homocoupling-free (Figure 1a). **Figure SI-6** further shows a series of six PCDTBT samples **1-6** with very similar weight average molecular weights  $M_{w,SEC} \sim 30$  kDa but with varying Cbz hc content. Obviously,  $\text{Pd}(\text{PPh}_3)_4$  was the only catalyst that enabled the preparation of hc-free PCDTBT samples **1**, **7** and **11** while all other catalytic systems led to Cbz hc contents of 2-8 mol-%. Also the commonly used combination of  $\text{Pd}_2\text{db}_3$ / phosphine ( $\text{P}(o\text{-tolyl})_3$  and SPHOS) led to clearly visible, albeit small amounts of 2 - 4 mol-% Cbz hc in PCDTBT **2**, **3**, **8**, **9**. Usage of the highly active Buchwald catalysts  $\text{Pd}_2\text{G}_3$  and  $\text{PdG}_2(o\text{-tolyl})_3\text{P}$  enabled the synthesis of PCDTBT **4** and **5** within minutes but led to significantly increased amounts of Cbz hc between 6-8 mol-% (Figure SI-6).

### 2.3 Steady-state spectroscopy and the establishment of a calibration curve

Having identified the fraction of homocoupled Cbz units for a variety of SPC conditions, we selected samples with constant molecular weight but varying Cbz hc content for further analysis of opto-electronic properties. Two series of samples, PCDTBT **1-6** with  $M_w \sim 30$  kDa and PCDTBT **7-10** with  $M_w \sim 60$  kDa both having Cbz hc contents of 0- 10 mol-% were chosen and investigated by steady-state absorption, photoluminescence spectroscopy and HOMO energy level determination via UPS (**Figure 2**). UV-vis absorption in chlorobenzene showed a clear reduction of the low-energy band (CT-like transition, see assignment next paragraph) with increasing Cbz hc content (Figure 2a). An increasing amount of Cbz hc can



correlate with a decreasing amount of TBT units in the chain, which can explain the linear decreases of the CT band cross section. Thus, correlating solution absorption properties with the content of Cbz hc appeared to be reasonable. Plotting the intensity ratio of the low and high energy absorption bands ( $I_{low}/I_{high}$ ) in the solution spectra versus mol-% Cbz hc gave a straight line that follows  $I_{low}/I_{high} = -0.02463 * \text{mol-\% Cbz hc} + 1.20371$  (Figure 2b). For MWs higher than  $M_w \sim 30$  kDa, the data points lie above this straight line, indicating that a saturation of the electronic conjugation length of PCDTBT in solution has not yet been reached (Figure 2b). From this straight line, Cbz homocoupling contents can easily be extracted for any sample without measuring and evaluating high temperature NMR measurements, and effects of molecular weight can be accounted for as well. The photoluminescence quantum efficiency (PLQE) in solution, excited at 532 nm, increased with Cbz hc, indicating that the perfectly alternating chain exhibits the lowest PLQE values (Figure 2c). This is fully congruent with statistical TBT copolymers which show increased PL values if the TBT unit is used as increasingly diluted comonomer.<sup>[30]</sup> Finally the HOMO energy level determined by UPS is found to slightly decrease with increasing Cbz hc, lying between -5.42 eV for defect-free PCDTBT **1** and -5.52 eV for PCDTBT **6** having 10 mol-% Cbz hc (Figure 2d).

## 2.4 DFT calculations

To get insight into the experimental photophysical properties, density functional theory (DFT) and time-dependent (TD)-DFT calculations were performed. The polymers are represented as finite size oligomers featuring four monomeric units.<sup>[31]</sup> The alternating chain is denoted as (Cbz-TBT)<sub>4</sub>, and the Cbz-Cbz hc and the TBT-TBT hc cases as (TBT-Cbz-TBT-Cbz-Cbz-TBT-Cbz-TBT) and (Cbz-TBT-Cbz-TBT-TBT-Cbz-TBT-Cbz), respectively. Although the TBT homocoupling defect is experimentally observed with very minor content, it is considered here to explore the impact of such kind of defects. This might be of interest as halide-halide homocoupling reactions have been observed recently, and hence should be

generally considered.<sup>[15]</sup> Two DFT functionals were employed, the hybrid B3LYP-D3 and the long-range separated LC-BLYP-D3 (range separated parameter optimized at  $\mu = 0.21$ ),<sup>[32]</sup> with inclusion of Grimme's dispersion corrections (D3),<sup>[33]</sup> and the 6-311G\* basis set. Both gas-phase and solvent-dependent (conductor polarizable continuum model CPCM with a dielectric constant for chlorobenzene of 5.6968) calculations were performed.<sup>[34]</sup> Charged species (+1) were fully optimized as well, and intra-molecular hole reorganization energies for the three cases (alternating, Cbz-Cbz hc and TBT-TBT hc) were computed at the LC-BLYP level of theory.<sup>[31]</sup> Because of their best match with the experimental data, we report the CPCM-LC-BLYP results here. All other computational results are given in the Supporting Information. All calculations were performed using Gaussian 09 revision D.01.<sup>[35]</sup> **Figure 3** shows the frontier molecular orbital isosurfaces (HOMO and LUMO) for the three cases. The HOMO topography is not affected by the hc defect, preserving its delocalized  $\pi$ -character over the oligomer length. The LUMO spatial distribution, intrinsically localized on the TBT unit (see alternating case), is however affected by the hc defect. In case of Cbz hc, the LUMO is localized on single TBT units, while for TBT hc it is delocalized over the two adjacent TBT units (Figure 3). Consequently, the molecular orbital energies (see Supporting Information) slightly vary for the HOMO ( $\pm 0.04$  eV), but are more sensitive for the LUMO ( $\pm 0.15$  eV) when going from the alternating to the Cbz-Cbz and TBT-TBT hc cases. **Figure 4** presents the excited state vertical transition energies and absorption spectra (CPCM-TD-DFT level) with band assignments. Two main absorption bands are identified: a low energy band (band A) mainly described as a HOMO-LUMO transition featuring a CT-like character (i.e. from  $\pi$ -delocalized to  $\pi^*$ -localized orbitals on the TBT unit), and a high energy band (band B) described as  $\pi$ - $\pi^*$  transitions delocalized over all the oligomer backbone. The TBT-TBT hc defect, more affecting the LUMO delocalization (Figure 3), induces a slight red shift of band A. In contrast, the Cbz hc defect decreases the oscillator strength of band A and leads to a

small blue shift of the transition energy, in accordance with the experimental UV-vis data.

The  $I_{\text{low}}/I_{\text{high}}$  intensity ratio decreases going from the alternating to the Cbz-Cbz hc defect species, also in good agreement with the observed data reported in Figure 2. This trend can be traced back to the fact that Cbz-Cbz hc defects increase localization of the LUMO, thus lowering the cross section of the CT-like transition.

## 2.5 Photovoltaic performance

Having identified and quantified Cbz homocoupling contents of various PCDTBT materials together with their influence on photophysical properties, we next turn to the question inasmuch such main chain defects affect solar cell performance. **Figure 5** and **Table 2** show current density- voltage ( $JV$ ) and external quantum efficiency (EQE) curves. Clearly, the short circuit current  $J_{\text{SC}}$  strongly decreased continuously with increasing Cbz hc content for both the 30 and 60 kDa series. The open circuit voltage remained approximately constant, in accordance with the only very slightly altered HOMO level (Table 2, Figure 2c). Comparing PCDTBT **1** (0 % hc) and PCDTBT **6** (10 % hc) within the 30 kDa series, the  $J_{\text{SC}}$  almost halved from 12.15 mA/cm<sup>2</sup> to 6.29 mA/cm<sup>2</sup>. Comparing PCDTBT **7** (0 % hc) and PCDTBT **10** (10 % hc) within the 60 kDa series, the  $J_{\text{SC}}$  dropped from 13.74 mA/cm<sup>2</sup> to 9.91 mA/cm<sup>2</sup>. The best performance was obtained from Cbz hc-free PCDTBT **7** with 60 kDa (highest PCE 7.17 %, average 6.85 %). While the shape of the  $JV$  curves representing the 60 kDa series is similar for PCDTBT **7**, **9** and **10**, PCDTBT **8** exhibits an exceptionally low fill factor as well as a reduced  $J_{\text{sc}}$ . We attribute this observation to the TBT hc formation observed in PCDTBT **8**. In addition, although not doubtlessly identified for PCDTBT **2**, we speculate TBT hc to be present in this sample as well. The strong reduction in the  $J_{\text{SC}}$  with increasing Cbz hc content cannot be explained by the reduced absorption of the charge-transfer band alone (see Figure SI-7 for blend film absorption), indicating that additional factors causing the lower OPV performance of defective PCDTBT are likely at play. Reorganization energies obtained from

DFT calculations on isolated oligomers, which can be considered as an important parameter for intramolecular charge transport, do not reveal major changes (see supporting information). However, as defects can induce changes in the inter-molecular charge transport properties, charge transport was carefully probed using field-effect transistor mobilities in bottom-contact top-gate geometry. We find the field-effect hole mobilities  $\mu_h$  of all PCDTBT samples within one order of magnitude, on the order of  $\sim 0.5$  to  $\sim 5 \times 10^{-3} \text{ cm}^2/\text{Vs}$  (Table 2 and Supporting Information). Under the same processing conditions, the  $M_w$  30 kDa series exhibits the highest  $\mu_h$  values for samples with none or limited Cbz hc:  $\mu_h = 2.87 \pm 0.24 \times 10^{-3} \text{ cm}^2/\text{Vs}$  and  $\mu_h = 4.22 \pm 0.24 \times 10^{-3} \text{ cm}^2/\text{Vs}$  are obtained for PCDTBT **1** (0 % Cbz hc) and PCDTBT **3** (3.6 % Cbz hc), respectively. On average, lower mobilities are observed for higher Cbz hc contents, but with no continuous trend: while a significantly lower  $\mu_h$  is measured for PCDTBT **4** with a Cbz hc content of 6% ( $0.527 \pm 0.022 \times 10^{-3} \text{ cm}^2/\text{Vs}$ ) and for PCDTBT **10** with 10 % ( $0.71 \pm 0.11 \times 10^{-3} \text{ cm}^2/\text{Vs}$ ),  $\mu_h$  is only smaller by a factor of 2 compared to the best mobility obtained for PCDTBT **5** (8 % Cbz hc,  $2.17 \pm 0.19 \times 10^{-3} \text{ cm}^2/\text{Vs}$ ). Overall the FET data indicate that reasonably good transport properties are obtained in all samples, with higher mobilities achieved for low contents of Cbz hc. While a direct comparison with PCE is not attempted because of the largely different operating conditions, subtle changes in charge transport are likely to be present in solar cells made with different polymer samples. However, given the absence of a continuous trend, we speculate that hole mobility may represent just one, possibly yielding a milder effect, of a set of interacting parameters leading to drastically reduced  $J_{SC}$  upon increasing defect concentration. In this context, the stronger localization of the LUMO on the TBT unit in the Cbz hc case compared to strictly alternating structures may lead to reduced exciton dissociation, which more strongly translates into reduced short circuit currents.<sup>[15]</sup>

The impact of Cbz hc defects on the photovoltaic performance of PCDTBT:PCBM blends is interesting in several aspects. First of all, the highest performance can be obtained when using defect-free PCDTBT. Secondly, considering main chain electronic defects as an additional parameter leads to better comparability of results and hence to a generally deeper understanding of structure-function relationships. To test this, we compare our OPV device efficiencies reported here with those reported by Kingsley *et al.*<sup>[29]</sup> Importantly, we used exactly the same device architecture, preparation conditions and hence a comparable layer thickness of ~80 nm. Figure SI-12 shows that the trend of a firstly increasing and then decreasing PCE with molecular weight of PCDTBT can be reproduced. Also in accordance with Kingsley *et al.*, we also find the chlorobenzene fraction with  $M_n \sim 22$  kDa to perform best. However when PCDTBT **7** ( $M_n \sim 23$  kDa, defect-free, chlorobenzene fraction) is compared to the chlorobenzene fraction used by Kingsley *et al.* (made by Pd<sub>2</sub>dba<sub>3</sub>/P(o-tolyl)<sub>3</sub>, hence likely to contain 4% of Cbz hc), a higher PCE is obtained (7.17 vs 6.15 %, respectively), revealing the beneficial effect of strictly alternating PCDTBT chains on photovoltaic performance. Looking at PCDTBT **9** (chlorobenzene fraction  $M_n$  28 kDa, 4 % Cbz hc) which has been made by the same reaction conditions as used by Kingsley *et al.*, the PCE drops to 6.15%, which is in excellent agreement. (see Figure SI-12). Importantly, the highest PCE exceeding 7% is only obtained with PCDTBT samples in which molecular weight is optimized *and* Cbz hc defects are eliminated. We note that higher PCE values for PCDTBT:PC<sub>71</sub>BM solar cells have been reported, but emphasize that the herein presented values stem from non-optimized devices made under conditions directly used from reference studies.

### 3. Conclusion

We have investigated the influence of carbazole homocoupling defects (Cbz hc) frequently occurring in PCDTBT samples made by Suzuki polycondensation on the opto-electronic properties. Cbz hc are quantified using high-temperature NMR spectroscopy assisted by

model compounds, are correlated with synthetic conditions and are finally fully eliminated to yield homocoupling-free materials. Correlation to UV-vis spectra enables a calibration curve from which the content of Cbz hc can be simply read out. Cbz hc strongly deteriorate the short circuit current and the device performance of photovoltaic cells. Interestingly, the majority of literature protocols for the synthesis of PCDTBT use conditions that lead to Cbz hc, hence the majority of PCDTBT samples used for OPV device testing may be defective as well. We believe that varying Cbz hc are one important factor responsible for poor reproducibility and comparability of different batches and results, and stress that next to molecular weight and molecular weight distribution electronic main chain defects must be considered to fully characterize, evaluate and compare results from conjugated polymers used in organic electronic devices.

### **Supporting Information**

Supporting Information is available from the Wiley Online Library or from the author.

### **Acknowledgements**

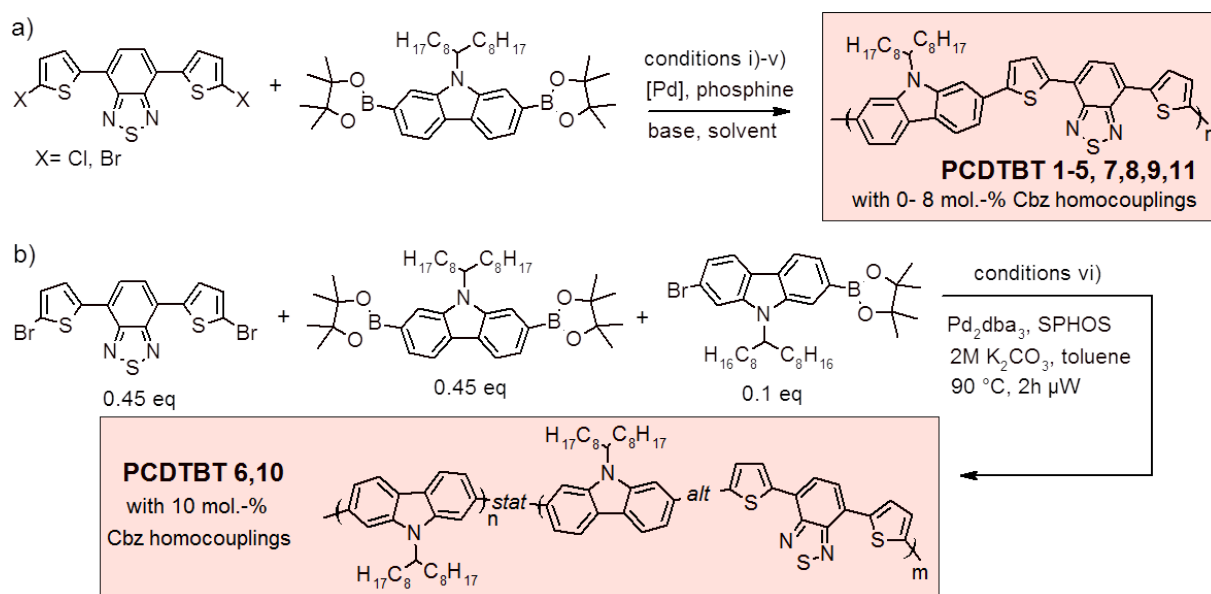
The authors thank M. Menke for fruitful discussions, A. Korwitz (IPF Dresden) for performing the HT-NMR measurements, A. Lederer and J. Lenz for performing some of the HT-SEC measurements, A. Mårtensson (Chalmers) for help with HT-SEC measurements, and A. Hasenhindl (University of Freiburg) for additional NMR measurements. F.L., M.S. and R.F. gratefully acknowledge the EPSRC for funding. M.S thanks the University of Freiburg (Innovationsfond Forschung) and the DFG for funding (SPP 1355). D.F. acknowledges the Alexander von Humboldt foundation for a postdoctoral research fellowship. A.D.Z.M. and C.M. thank the Swedish Research Council for funding. D.N. and M.C. acknowledge the financial support by the European Research Council (ERC) under the European Union's Horizon 2020 research and innovation program "HEROIC", grant agreement 638059.

### **References**

- [1] L. Dou, J. You, Z. Hong, Z. Xu, G. Li, R. A. Street, Y. Yang, *Adv. Mater.* **2013**, *25*, 6642.
- [2] H. Sirringhaus, *Adv. Mater.* **2014**, *26*, 1319.
- [3] L. Ying, C.-L. Ho, H. Wu, Y. Cao, W.-Y. Wong, *Adv. Mater.* **2014**, *26*, 2459.

- [4] P. Heremans, G. H. Gelinck, R. Müller, K.-J. Baeg, D.-Y. Kim, Y.-Y. Noh, *Chem. Mater.* **2011**, *23*, 341.
- [5] Q. Zhang, Y. Sun, W. Xu, D. Zhu, *Adv. Mater.* **2014**, *26*, 6829.
- [6] Y.-J. Cheng, S.-H. Yang, C.-S. Hsu, *Chem. Rev.* **2009**, *109*, 5868.
- [7] Y. He, W. Hong, Y. Li, *J. Mater. Chem. C* **2014**, *2*, 8651.
- [8] K. C. Kong, C. H. Cheng, *J. Am. Chem. Soc.* **1991**, *113*, 6313.
- [9] R. van Asselt, C. J. Elsevier, *Organometallics* **1994**, *13*, 1972.
- [10] A. Lei, X. Zhang, *Tetrahedron Lett.* **2002**, *43*, 2525.
- [11] C. Adamo, C. Amatore, I. Ciofini, A. Jutand, H. Lakmini, *J. Am. Chem. Soc.* **2006**, *128*, 6829.
- [12] W. D. Miller, A. H. Fray, J. T. Quatroche, C. D. Sturgill, *Org. Process Res. Dev.* **2007**, *11*, 359.
- [13] P. Kohn, S. Huettner, H. Komber, V. Senkovskyy, R. Tkachov, A. Kiriya, R. H. Friend, U. Steiner, W. T. S. Huck, J.-U. Sommer, M. Sommer, *J. Am. Chem. Soc.* **2012**, *134*, 4790.
- [14] F. Koch, W. Heitz, *Macromol. Chem. Phys.* **1997**, *198*, 1531.
- [15] K. H. Hendriks, W. Li, G. H. L. Heintges, G. W. P. van Pruissen, M. M. Wienk, R. A. J. Janssen, *J. Am. Chem. Soc.* **2014**, *136*, 11128.
- [16] F. Lombeck, R. Matsidik, H. Komber, M. Sommer, *Macromol. Rapid Commun.* **2015**, *36*, 231.
- [17] F. Lombeck, H. Komber, S. I. Gorelsky, M. Sommer, *ACS Macro Lett.* **2014**, 819.
- [18] S. Kowalski, S. Allard, U. Scherf, *Macromol. Rapid Commun.* **2015**, *36*, 1061.
- [19] S. Broll, F. Nübling, A. Luzio, D. Lentzas, H. Komber, M. Caironi, M. Sommer, *Macromolecules* **2015**, *48*, 7481.
- [20] A. E. Rudenko, B. C. Thompson, *J. Polym. Sci. Part Polym. Chem.* **2014**, n/a.
- [21] W. Hong, S. Chen, B. Sun, M. A. Arnould, Y. Meng, Y. Li, *Chem. Sci.* **2015**, *6*, 3225.
- [22] T. Vangerven, P. Verstappen, J. Drijkoningen, W. Dierckx, S. Himmelberger, A. Salleo, D. Vanderzande, W. Maes, J. V. Manca, *Chem. Mater.* **2015**, *27*, 3726.
- [23] S. H. Park, A. Roy, S. Beaupré, S. Cho, N. Coates, J. S. Moon, D. Moses, M. Leclerc, K. Lee, A. J. Heeger, *Nat. Photonics* **2009**, *3*, 297.
- [24] N. Blouin, A. Michaud, M. Leclerc, *Adv. Mater.* **2007**, *19*, 2295.
- [25] S. Beaupré, M. Leclerc, *J. Mater. Chem. A* **2013**, *1*, 11097.
- [26] C. H. Peters, I. T. Sachs-Quintana, J. P. Kastrop, S. Beaupré, M. Leclerc, M. D. McGehee, *Adv. Energy Mater.* **2011**, *1*, 491.
- [27] W. R. Mateker, I. T. Sachs-Quintana, G. F. Burkhard, R. Cheacharoen, M. D. McGehee, *Chem. Mater.* **2015**, *27*, 404.
- [28] N. C. Bruno, M. T. Tudge, S. L. Buchwald, *Chem. Sci.* **2013**, *4*, 916.
- [29] J. W. Kingsley, P. P. Marchisio, H. Yi, A. Iraqi, C. J. Kinane, S. Langridge, R. L. Thompson, A. J. Cadby, A. J. Pearson, D. G. Lidzey, R. A. L. Jones, A. J. Parnell, *Sci. Rep.* **2014**, *4*, DOI 10.1038/srep05286.
- [30] Q. Hou, Y. Xu, W. Yang, M. Yuan, J. Peng, Y. Cao, *J. Mater. Chem.* **2002**, *12*, 2887.
- [31] A. Luzio, D. Fazzi, F. Nübling, R. Matsidik, A. Straub, H. Komber, E. Giussani, S. E. Watkins, M. Barbatti, W. Thiel, E. Gann, L. Thomsen, C. R. McNeill, M. Caironi, M. Sommer, *Chem. Mater.* **2014**, *26*, 6233.
- [32] K. Sen, R. Crespo-Otero, O. Weingart, W. Thiel, M. Barbatti, *J. Chem. Theory Comput.* **2013**, *9*, 533.
- [33] S. Grimme, S. Ehrlich, L. Goerigk, *J. Comput. Chem.* **2011**, *32*, 1456.
- [34] M. Cossi, N. Rega, G. Scalmani, V. Barone, *J. Comput. Chem.* **2003**, *24*, 669.
- [35] Gaussian 09, Revision D.01, M. J. Frisch, G. W. Trucks, H. B. Schlegel, G. E. Scuseria, M. A. Robb, J. R. Cheeseman, G. Scalmani, V. Barone, B. Mennucci, G. A. Petersson, H. Nakatsuji, M. Caricato, X. Li, H. P. Hratchian, A. F. Izmaylov, J. Bloino, G. Zheng, J. L. Sonnenberg, M. Hada, M. Ehara, K. Toyota, R. Fukuda, J. Hasegawa,

M. Ishida, T. Nakajima, Y. Honda, O. Kitao, H. Nakai, T. Vreven, J. A. Montgomery, Jr., J. E. Peralta, F. Ogliaro, M. Bearpark, J. J. Heyd, E. Brothers, K. N. Kudin, V. N. Staroverov, R. Kobayashi, J. Normand, K. Raghavachari, A. Rendell, J. C. Burant, S. S. Iyengar, J. Tomasi, M. Cossi, N. Rega, J. M. Millam, M. Klene, J. E. Knox, J. B. Cross, V. Bakken, C. Adamo, J. Jaramillo, R. Gomperts, R. E. Stratmann, O. Yazyev, A. J. Austin, R. Cammi, C. Pomelli, J. W. Ochterski, R. L. Martin, K. Morokuma, V. G. Zakrzewski, G. A. Voth, P. Salvador, J. J. Dannenberg, S. Dapprich, A. D. Daniels, Ö. Farkas, J. B. Foresman, J. V. Ortiz, J. Cioslowski, and D. J. Fox, Gaussian, Inc., Wallingford CT, 2009.



**Scheme 1.** a) Synthesis of PCDTBT under varying Suzuki polycondensation conditions and (b) with intentionally introduced Cbz hc defects. Reaction conditions: i) X = Br, Pd(PPh<sub>3</sub>)<sub>4</sub>, 2M K<sub>2</sub>CO<sub>3</sub>, toluene, 90 °C, 2d; ii) X= Br, Pd<sub>2</sub>dba<sub>3</sub>/ phosphine (SPHOS or P(o-tol)<sub>3</sub>), 2M K<sub>2</sub>CO<sub>3</sub>, toluene, 90 °C, 2d, iii) X= Cl, Pd<sub>2</sub>dba<sub>3</sub>/ SPHOS, 2M K<sub>2</sub>CO<sub>3</sub>, toluene, 80 °C, 2d, iv) X= Br, Pd<sub>2</sub>G<sub>3</sub>/ SPHOS, 2M K<sub>2</sub>CO<sub>3</sub>, toluene, 90 °C, 20min, v) X= Br, PdG<sub>2</sub>(o-toly)<sub>3</sub>P, 2M K<sub>2</sub>CO<sub>3</sub>, toluene, 90 °C, 20min; vi) Pd<sub>2</sub>dba<sub>3</sub>/ SPHOS, 2M K<sub>2</sub>CO<sub>3</sub>, toluene, 3h, 90°C, microwave-assisted heating.



**Table 1.** Overview of PCDTBT samples used in this study.

	#	method <sup>a)</sup>	Cat	$M_n/M_w$ [kDa] <sup>b)</sup>	Cbz hc <sup>c)</sup>	Ratio $I_{\pi\pi^*}/I_{n\pi^*}$ <sup>d)</sup>
M <sub>w</sub> ~30 kDa	1	i <sup>e</sup>	Pd[PPh <sub>3</sub> ] <sub>4</sub>	CF: 8/32	0	CF: 1.195
	2	ii <sup>e</sup>	Pd <sub>2</sub> dba <sub>3</sub> SPHOS	CF: 10/33	2.4	CF: 1.149
	3	iii <sup>f</sup>	Pd <sub>2</sub> dba <sub>3</sub> SPHOS	CF: 12/33	3.6	CF: 1.113
	4	iv <sup>e</sup>	Pd <sub>2</sub> G <sub>3</sub> SPHOS	CF: 7/35	6.0	CF: 1.064
	5	v <sup>e</sup>	PdG <sub>2</sub> ( <i>o</i> -tol) <sub>3</sub> P	CF: 10/30	8.0	CF: 1.024
	6	vi	Pd <sub>2</sub> dba <sub>3</sub> SPHOS	CF: 12/43	10.0	CF: 0.985
M <sub>w</sub> ~60 kDa	7	i <sup>f</sup>	Pd[PPh <sub>3</sub> ] <sub>4</sub>	CB: 23/72	0	CB: 1.251
	8	iii <sup>e</sup>	Pd <sub>2</sub> dba <sub>3</sub> SPHOS	CF: 15/48	2.5	CF: 1.089
	9	ii <sup>e</sup>	Pd <sub>2</sub> dba <sub>3</sub> P( <i>o</i> -tol) <sub>3</sub>	CB: 28/58	4.0	CB: 1.158
	10	vi <sup>e</sup>	Pd <sub>2</sub> dba <sub>3</sub> SPHOS	CB: 21/52	10.0	CB: 0.975
M <sub>w</sub> ~80 kDa	11	i <sup>e</sup>	Pd[PPh <sub>3</sub> ] <sub>4</sub>	CB: 25/81	0	CB: 1.279

<sup>a)</sup> for synthetic methods see caption Scheme 1; <sup>b)</sup> obtained from high temperature SEC in TCB at 150 °C, <sup>c)</sup> from <sup>1</sup>H NMR spectroscopy, <sup>d)</sup> ratio of absorption bands in chlorobenzene at 0.02 mg/ml, <sup>e)</sup>90 °C reaction temperature, <sup>f)</sup>80 °C reaction temperature. CF and CB indicate chloroform and chlorobenzene fractions, respectively.

**Table 2.** Overview of solar cell and OFET parameters; average values are given, characteristics of the best cell is given in brackets. n.d. not determined

	#	$J_{sc}/ \text{mA}/\text{cm}^2$	$V_{oc}$ [V]	FF	PCE [%]	$\mu_{h,OFET} \times 10^{-3}$ [ $\text{cm}^2/\text{Vs}$ ]
<b>Mw ~30 kDa</b>	<b>1</b>	$12.15 \pm 0.43$	$0.86 \pm 0.02$	$0.50 \pm 0.02$	$5.22 \pm 0.53$ (5.78)	$2.87 \pm 0.24$
	<b>2</b>	$12.63 \pm 0.48$	$0.83 \pm 0.02$	$0.34 \pm 0.04$	$3.56 \pm 0.26$ (3.79)	n.d.
	<b>3</b>	$11.05 \pm 0.29$	$0.88 \pm 0.02$	$0.41 \pm 0.02$	$3.97 \pm 0.16$ (4.12)	$4.22 \pm 0.41$
	<b>4</b>	$9.43 \pm 0.50$	$0.86 \pm 0.01$	$0.50 \pm 0.04$	$4.05 \pm 0.28$ (4.27)	$0.527 \pm 0.022$
	<b>5</b>	$9.75 \pm 0.62$ (10.37)	$0.86 \pm 0.03$ (0.89)	$0.37 \pm 0.02$ (0.38)	$3.10 \pm 0.41$ (3.51)	$2.17 \pm 0.19$
	<b>6</b>	$6.29 \pm 0.68$	$0.81 \pm 0.04$	$0.36 \pm 0.03$	$1.83 \pm 0.31$ (2.05)	n.d.
<b>Mw ~60 kDa</b>	<b>7</b>	$13.12 \pm 0.62$ (13.74)	$0.87 \pm 0.01$ (0.87)	$0.60 \pm 0.02$ (0.60)	$6.85 \pm 0.32$ (7.17)	$2.63 \pm 0.42$
	<b>8</b>	$11.17 \pm 0.32$ (11.49)	$0.88 \pm 0.01$ (0.88)	$0.44 \pm 0.03$ (0.47)	$4.38 \pm 0.17$ (4.75)	n.d.
	<b>9</b>	$12.78 \pm 0.39$ (13.17)	$0.88 \pm 0.01$ (0.88)	$0.53 \pm 0.02$ (0.55)	$6.15 \pm 0.13$ (6.28)	$5.30 \pm 0.15$
	<b>10</b>	$9.91 \pm 0.26$ (10.09)	$0.90 \pm 0.02$ (0.91)	$0.47 \pm 0.02$ (0.48)	$4.19 \pm 0.21$ (4.40)	$0.71 \pm 0.11$
<b>Mw ~80 kDa</b>	<b>11</b>	$12.62 \pm 0.39$ (12.99)	$0.88 \pm 0.02$ (0.89)	$0.54 \pm 0.02$ (0.55)	$5.99 \pm 0.36$ (6.35)	n.d.

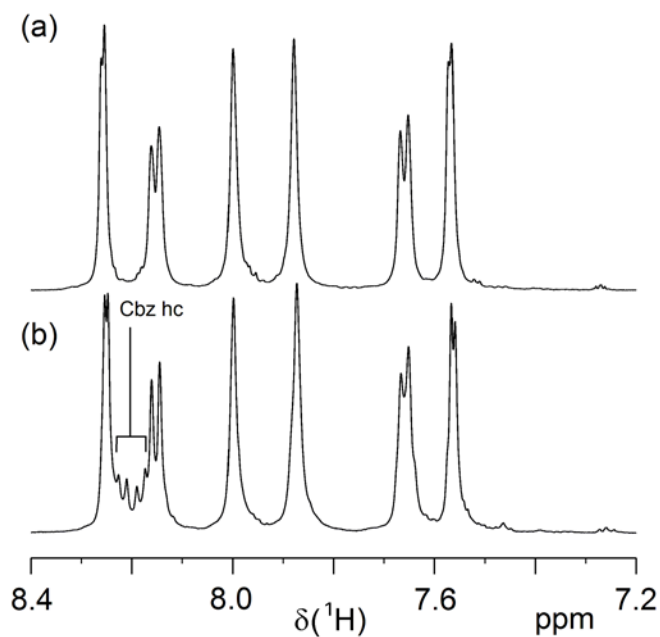


**Figure 1.**  $^1\text{H}$  NMR spectra of PCDTBT **7** (a) and **6** (b) with 0 and 10 mol% Cbz hc, respectively, in  $\text{C}_2\text{D}_2\text{Cl}_4$  at  $120\text{ }^\circ\text{C}$ .

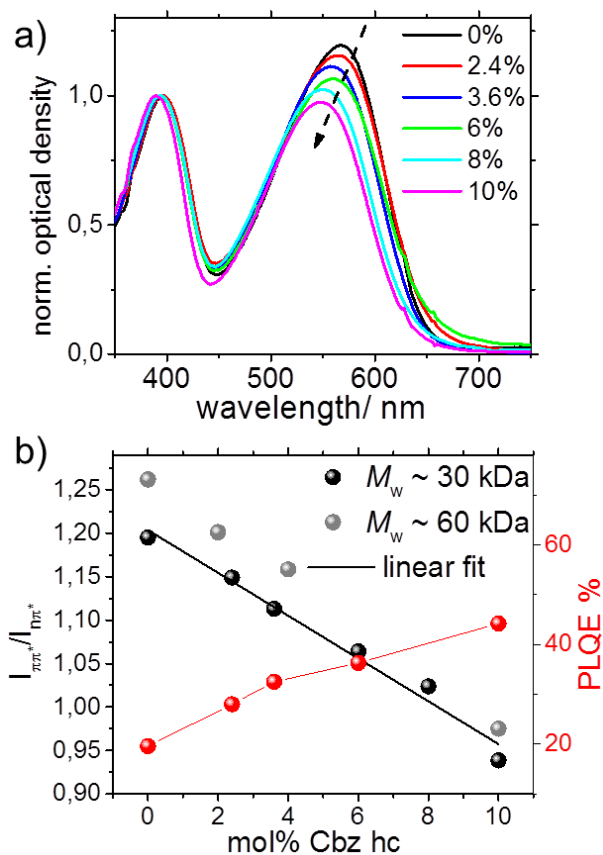


**Figure 2.** Optical properties of PCDTBT as a function of the Cbz homocoupling content. a) UV-vis absorption in chlorobenzene (PCDTBT **1-6**) and b) ratio of absorption bands with linear fit and photoluminescence quantum efficiency (PLQE).

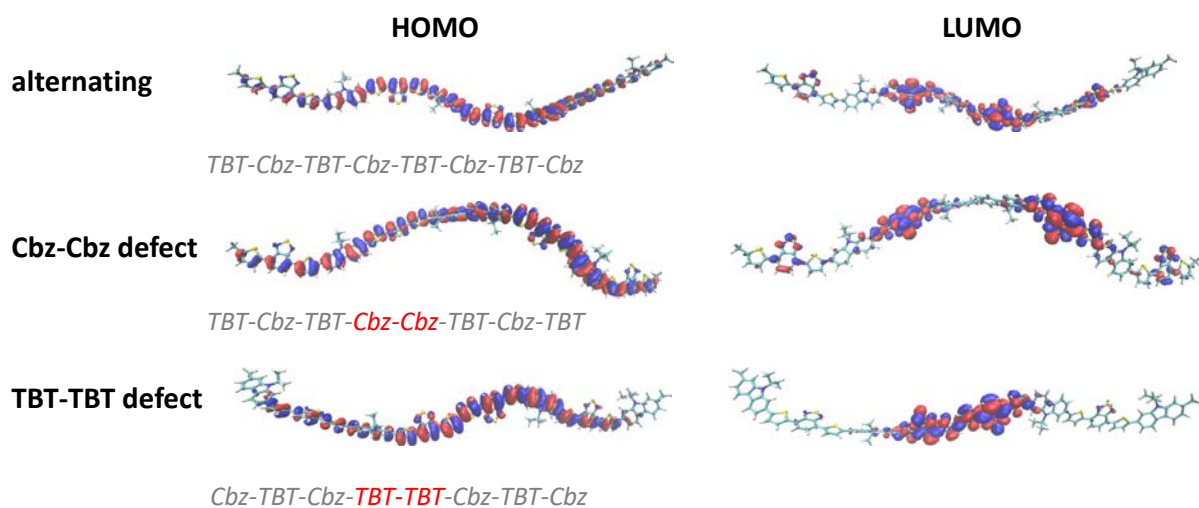


**Figure 3.** DFT (CPCM-LC-BLYP/6-311G\*) frontier molecular orbitals (HOMO and LUMO) for alternating, Cbz-Cbz and TBT-TBT hc defect cases.

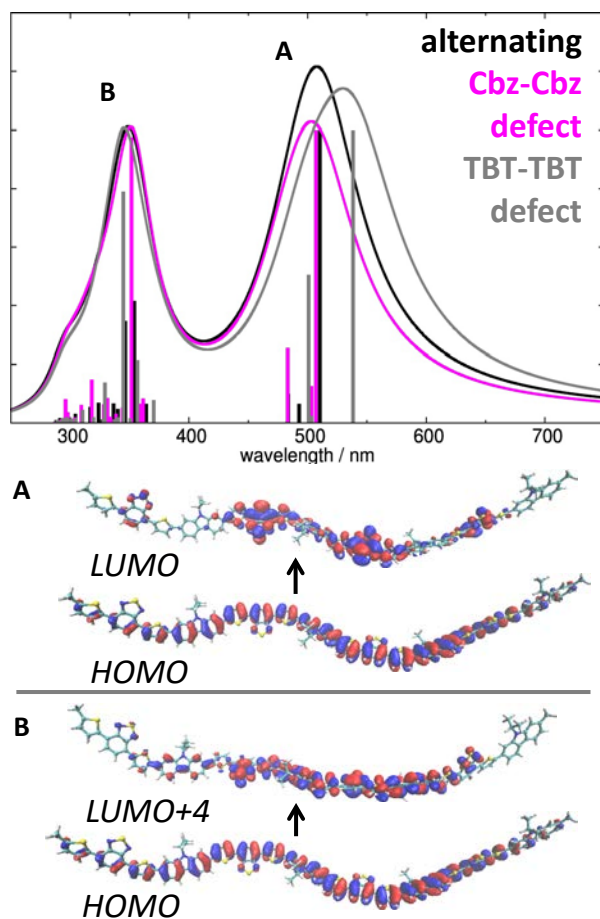


**Figure 4.** Left: TD-DFT(CPCM-LC-BLYP/6-311G\*) vertical transitions and absorption spectra (convolution of Lorentzian functions, FWHM = 0.2 eV) for alternating, Cbz-Cbz and TBT-TBT hc defect cases. Right: Assignments of molecular orbitals (alternating PCDTBT; for orbitals of Cbz-Cbz and TBT-TBT hc see Supporting Information) of the low energy absorption band A and of the high energy band B.

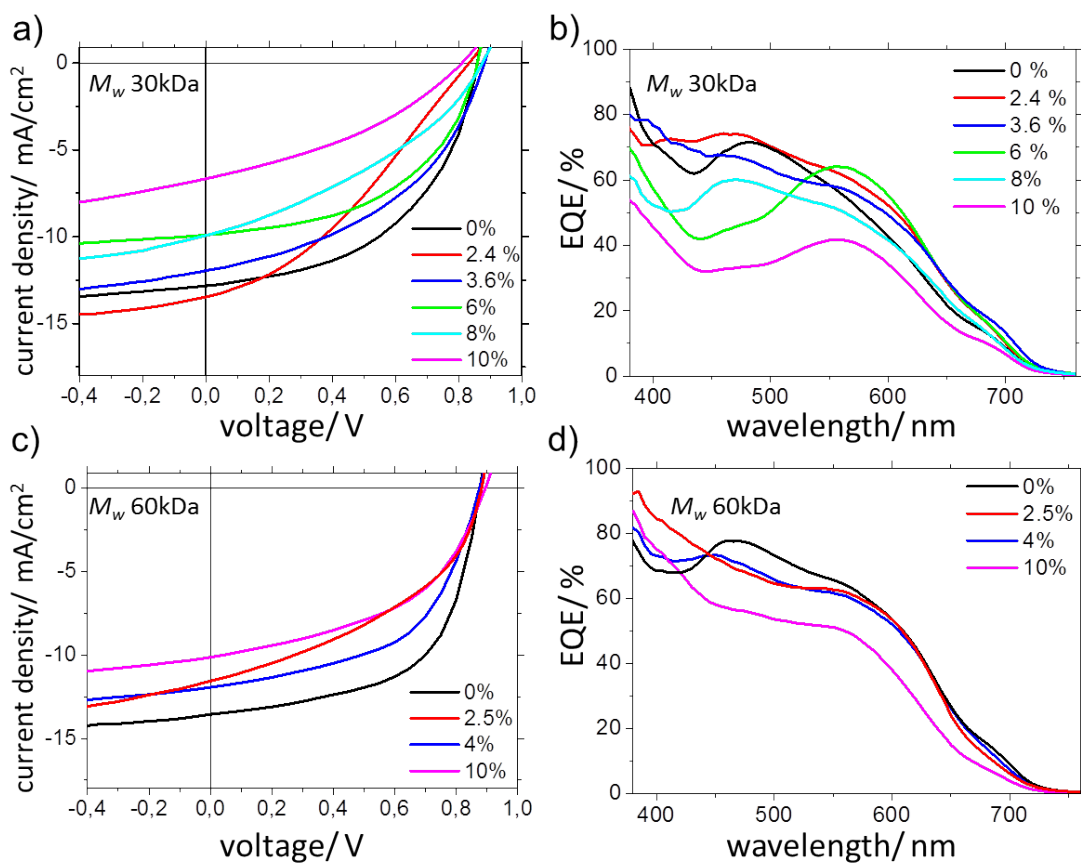


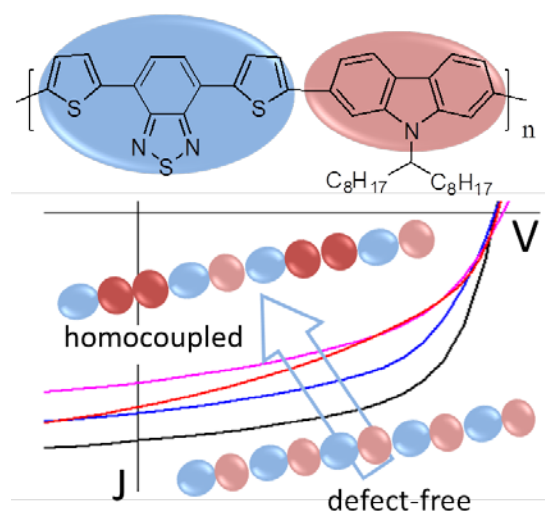
**Figure 5.** Solar cells characteristics of PCDTBT:PC<sub>71</sub>BM blends with varying Cbz hc content. a)  $J-V$  curves and b) respective external quantum efficiencies (EQE) of PCDTBT ( $M_w \sim 30\text{kDa}$ ) **1** (0%), **2** (2.4%), **3** (3.6%), **4** (6%) **5** and **6** (10%). c)  $J-V$  curves and d) respective external quantum efficiencies of PCDTBT ( $M_w \sim 60\text{kDa}$ ) **7** (0%) **8** (2.5%), **9** (4%) and **10** (10%).

**Electronic main chain defects in conjugated polymers caused by carbazole homocouplings (Cbz hc) significantly deteriorate the performance of organic photovoltaics (OPV) as shown for PCDTBT:PC<sub>71</sub>BM devices. Cbz hc occur frequently, are quantified for a variety of Suzuki conditions and are correlated with photophysical properties. PCDTBT without main chain defects *and* optimized molar mass gives the highest PCEs exceeding 7 %. Main chain electronic defects must be considered to enable comparability and reproducibility of OPV devices in which conjugated polymers are used.**

Organic solar cells

*F. Lombeck, H. Komber, D. Fazzi, D. Nava, J. Kuhlmann, D. Stegerer, K. Strassel, J. Brandt, A. Diaz de Zerio Mendaza, C. Müller, W. Thiel, M. Caironi, R. Friend, M. Sommer\**

**On the effect of prevalent carbazole homocouplings on the photovoltaic performance of PCDTBT:PC<sub>71</sub>BM solar cells**



((Supporting Information can be included here using this template))

Copyright WILEY-VCH Verlag GmbH & Co. KGaA, 69469 Weinheim, Germany, 2013.

## Supporting Information

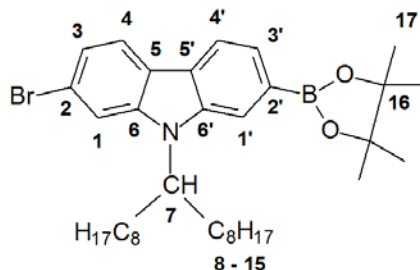
### On the effect of prevalent carbazole homocouplings on the photovoltaic performance of PCDTBT:PC71BM solar cells

#### Materials

All chemicals were purchased from Sigma-Aldrich. 2-Isopropoxy-4,4,5,5-tetramethyl-1,3,2-dioxaborolane (98%) was purchased from ABCR. The monomers were synthesized according to the literature.<sup>1,2</sup>

#### 2-Bromo-9-(heptadecan-9-yl)-7-(4,4,5,5-tetramethyl-1,3,2-dioxaborolan-2-yl)-9H-carbazole (Br-Cbz-Bpin).

N-9'-Heptadecanyl-2,7-dibromocarbazole (CbzBr<sub>2</sub>, 0.36 g, 0.63 mmol) were placed in a Schlenk tube and dissolved in 15 ml dry THF. The solution was cooled to -78°C in a dry ice bath. *n*-Butyl lithium (0.26 ml, 2.5 M in heptane) was added dropwise. The reaction mixture was stirred at -78°C for 2 h. 2-Isopropoxy-4,4,5,5-tetramethyl-1,3,2-dioxaborolane (0.28 ml, 1.01 mmol) was added. The reaction mixture was allowed to warm to RT overnight. Water (20 ml) was added and the crude product was extracted with diethyl ether three times. The organic phase was combined and dried over magnesium sulfate. The solvent was removed. The product was obtained as colorless oil (191 mg, 0.327 mmol, 52% after column chromatography with *iso*-hexanes:ethyl acetate 19:1).



<sup>1</sup>H NMR (CDCl<sub>3</sub>, 30°C): δ = 8.2 – 7.8 (br, 4H; 1', 4, 4'), 7.71 and 7.54 (s, 1H; 1), 7.68 (d, 1H; 3'), 7.31 (d, 1H, 3), 4.66 and 4.44 (br, 1H; 7), 2.33, 2.20 and 1.93 (br, 4H; 8), 1.40 (s, 12H; 17), 1.4 – 0.9 (24H; 9-14), 0.83 ppm (t, 6H; 15); several signals show a splitting due to two rotamers resulting from slow rotation about C-N bond.



$^{13}\text{C}$  NMR ( $\text{CDCl}_3$ ,  $30^\circ\text{C}$ ):  $\delta = 143.2$  (6, minor (mi) rotamer),  $141.6$  ( $6'$ , major (ma) rotamer),  $139.8$  (6, ma),  $138.3$  ( $6'$ , mi),  $126.2$  (br,  $2'$ );  $125.8$  ( $5'$ , mi),  $125.3$  ( $3'$ ),  $124.4$  ( $5'$ , ma),  $122.6$  (5, ma),  $121.9$  (4, ma),  $121.7$  (3; 4, mi),  $121.2$  (5, mi),  $119.9$  (2, mi),  $119.6$  ( $4'$ , mi),  $119.4$  (2, ma;  $4'$ , ma),  $118.1$  ( $1'$ , mi),  $115.4$  ( $1'$ , ma),  $114.4$  (1, ma),  $112.0$  (1, mi),  $83.8$  (16),  $57.0$  (7, mi),  $56.3$  (7, ma),  $33.6$  (8),  $31.7$  (13),  $29.4$  (10),  $29.3$  and  $29.1$  (11; 12),  $26.7$  (9),  $24.9$  (17),  $22.6$  (14),  $14.0$  ppm (15).

$^1\text{H}$  NMR ( $\text{C}_2\text{D}_2\text{Cl}_4$ ,  $120^\circ\text{C}$ ):  $\delta = 8.06$  (d, 1H; 4),  $7.99$  (s, 1H;  $1'$ ),  $7.98$  (d, 1H; 4);  $7.72$  (d, 1H;  $3'$ ),  $7.69$  (s, 1H; 1),  $7.36$  (dd, 1H, 3),  $4.62$  (m, 1H; 7),  $2.31$  and  $2.03$  (m, 4H; 8),  $1.45$  (s, 12H; 17),  $1.4 - 1.1$  (24H; 9-14),  $0.90$  ppm (t, 6H; 15).

$^{13}\text{C}$  NMR ( $\text{C}_2\text{D}_2\text{Cl}_4$ ,  $120^\circ\text{C}$ ):  $\delta = 141.4$  (br; 6),  $140.3$  (br;  $6'$ ),  $126.7$  (br,  $2'$ );  $125.2$  ( $3'$ ),  $124.8$  ( $5'$ ),  $122.0$  (5),  $121.5$  (3),  $121.3$  (4),  $119.3$  (2),  $118.9$  ( $4'$ ),  $116.6$  (br;  $1'$ ),  $113.2$  (br; 1),  $83.4$  (16),  $56.5$  (7),  $33.6$  (8),  $31.3$  (13),  $28.9$ ,  $28.8$  and  $28.6$  (10 - 12),  $26.5$  (9),  $24.6$  (17),  $22.1$  (14),  $13.4$  ppm (15).

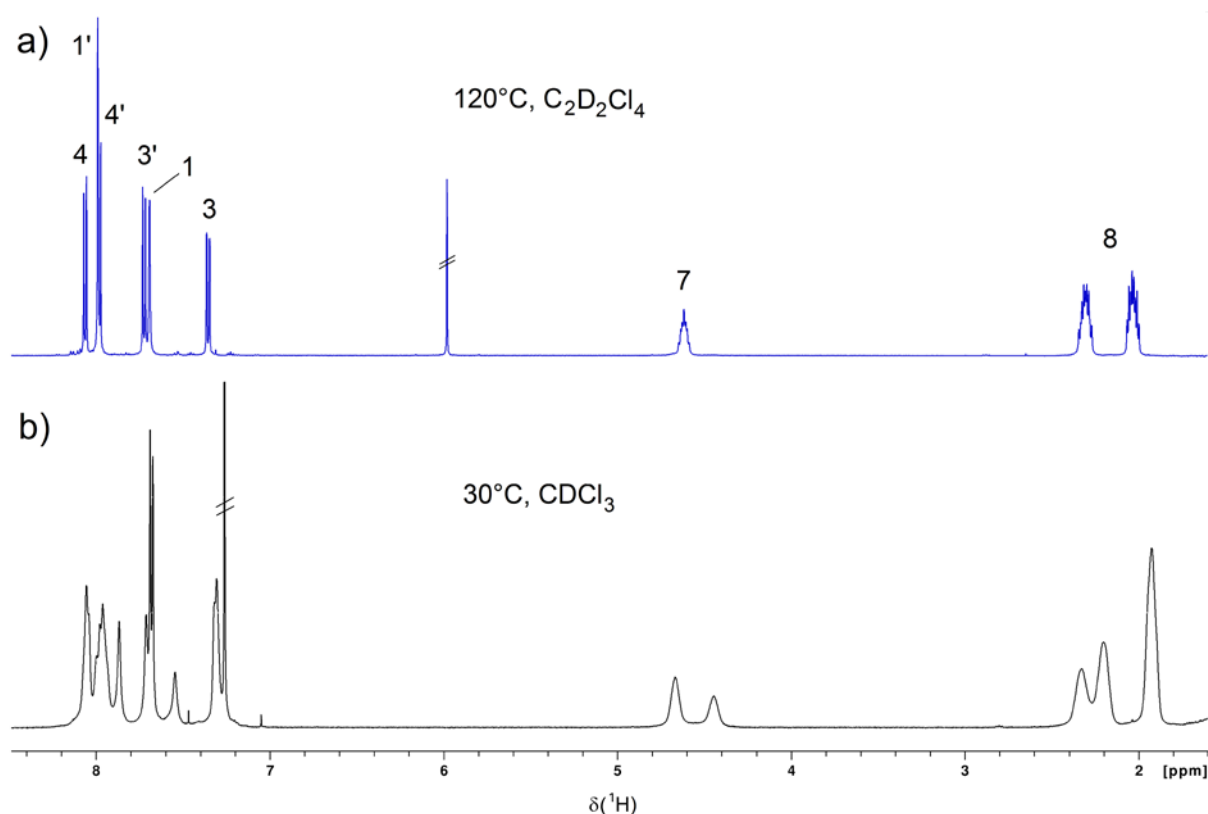


**Figure SI-1.**  $^1\text{H}$  NMR spectra of Br-Cbz-BPin at  $120^\circ\text{C}$  in  $\text{C}_2\text{D}_2\text{Cl}_4$  (a) with fast rotation of the alkyl group around the C-N bond and at  $30^\circ\text{C}$  in  $\text{CDCl}_3$  (b) with slow rotation resulting in signal broadening or separate signals for major rotamer and minor rotamer.

### General synthesis of PCDTBT.

**Br<sub>2</sub>TBT** (46.8 mg, 0.102 mmol), **Cbz(Bpin)<sub>2</sub>** (67.2 mg, 0.102 mmol) were placed in a screw cap vial. The catalyst (palladium precursor (1 mol% Pd) and phosphine (2 mol%)) was added in an argon-filled glovebox. Degassed toluene, 2 M K<sub>2</sub>CO<sub>3</sub> (1:1 v/v) and 1 drop of Aliquat 336® were added to give a monomer concentration of 0.1 M. The vial was sealed with a Teflon cap and the mixture stirred at 80°C for 3d. The mixture was allowed to cool to RT, 10 ml 1,2-dichlorobenzene were added and the resulting polymer was precipitated into methanol, filtered and washed by subsequent Soxhlet extraction with methanol, acetone, iso-hexanes, chloroform and chlorobenzene. For molecular weights of  $M_w \sim 30$  kDa, the chloroform fraction was used whereas the chlorobenzene fractions exhibited  $M_w \sim 60$  kDa. The chloroform and chlorobenzene fraction were collected, poured into methanol, collected by centrifugation and dried under reduced pressure to give the polymer as a deep purple solid in 40-89% yield.

### Instrumentation

*NMR spectroscopy.* <sup>1</sup>H (500.13 MHz) and <sup>13</sup>C (125.77 MHz) NMR spectra were recorded on a Bruker Avance III 500 spectrometer using a 5 mm <sup>1</sup>H/<sup>13</sup>C/<sup>19</sup>F/<sup>31</sup>P gradient probe and on a Bruker Avance II 300 at 299.87 MHz (<sup>1</sup>H) and 75.40 MHz (<sup>13</sup>C). CDCl<sub>3</sub> was used as solvent, lock and internal standard ( $\delta(^1\text{H}) = 7.26$  ppm;  $\delta(^{13}\text{C}) = 77.0$  ppm). The 500.13 MHz <sup>1</sup>H NMR spectra of all copolymer samples were recorded at 120°C using C<sub>2</sub>D<sub>2</sub>Cl<sub>4</sub> as solvent and were referenced to the residual solvent peak ( $\delta(^1\text{H}) = 5.98$  ppm).

*High temperature size exclusion Chromatography (HT-SEC).* HT-SEC was performed on a PL GPC 220 (Agilent Laboratories, US) using 2xMixed-B-LS PLgel, 300 x 7,5 mm columns packed with 10  $\mu\text{m}$  particles (Agilent Laboratories, US). As a solvent 1,2,4-trichlorobenzene, (stabilized with 1 g/L BHT) with a flow rate of 1 mL/min was used. Detection was done with an integrated dRI-detector, operating at 890 nm, a UV-Vis-detector (200 - 750 nm, Testa

Analytical Solutions e.K., DE) with a column oven integrated flow cell and for universal calibration a viscosity detector (PL-BV 400 Series). All measurements were carried out at 150 °C. The molar masses were calculated with both relative and universal calibration, using polystyrene standards. Usage of the UV-detector enabled the analysis of small amounts of sample (~ 0.15 mg/ml).

*UV-vis spectroscopy.* UV-vis spectra were recorded on a Lambda 650 S spectrometer from Perkin Elmer in film or in chlorobenzene solutions ( $c = 0.02$  mg/ml).

*Photoluminescence quantum efficiency.* The measurement is carried out on films deposited on quartz glass (Spectrosil 2000) or chlorobenzene solutions (0.02 mg/ml) in a Hellma quartz cuvette (1 mm beam path) via excitation of the sample with a 523 nm laser. The sample is placed inside an integrating sphere. The integrating sphere's inside is reflective and purged with nitrogen. The light collected from the integrating sphere is coupled through a fiber into a spectrometer (Shamrock SR303i, Andor Technologies). Three individual measurements were performed to calculate the quantum yield  $\phi$  according to DE MELLO *et al.*<sup>4</sup> In the ON measurement the laser is focused on the film directly, whereas in the OFF measurement the laser does not hit the sample but the reflective wall of the integrating sphere. The background is subtracted by measuring the integrating sphere without sample to account for impurities inside the sphere. The PLQE is calculated by the difference in the area of the laser peak of all three measurements, which gives the amount of photons absorbed by the film, and the difference in the signal area of the emission peak, giving the number of photons emitted.

*Ultraviolet photoelectron spectroscopy.* For UPS measurements 7 nm of chromium and 70 nm of gold were evaporated on top of a clean silicon substrate. The ~10 nm - 15 nm thin polymer film was deposited via spin coating. After thermal annealing at 160°C for 10min. in a

nitrogen-filled glovebox, the films were transferred into an ultrahigh vacuum chamber (ESCALAB 250Xi). UPS measurements were carried out using a pumped He gas discharge lamp emitting He I radiation ( $h\nu = 21.2$  eV).

*OPV device fabrication.* Photovoltaic devices were fabricated in the standard ITO|PEDOT:PSS|PCDTBT:PC<sub>71</sub>BM(1:4)|Ca/Al layer sequence. ITO on glass anodes were first cleaned with toluene, acetone and isopropanol, followed by ultrasonic in the same solvents and oxygen plasma treatment. A ~40 nm thick PEDOT:PSS was spin-coated onto the plasma-treated substrates, annealed at 160 °C for 20 min. The blend solution was prepared by mixing 250  $\mu$ l PCDTBT (12 mg/ml in 1,2-dichlorobenzene) and 250  $\mu$ l PC<sub>71</sub>BM (48 mg/ml in 1,2-dichlorobenzene). Photoactive layers were spin-cast in air from 1,2-dichlorobenzene-solution (PCDTBT:PC<sub>71</sub>BM 1:4) at 65°C to give 95-110 nm thick films. The coated substrates were transferred into an evaporation and kept at  $\sim 10^{-7}$  mbar overnight prior to deposition of the Ca (2.5 nm)/Al(100 nm) electrode.

Film thicknesses were determined *via* AFM profile measurement of a scraped film with an average film-to-film deviation of  $\pm 6$  nm. AFM measurements were carried out in a Veeco Dimension 3100 AFM, operated in tapping mode. The film thicknesses were corrected in respect to the PEDOT:PSS layer underneath.

*Device testing.* Device EQE was measured using a tungsten lamp with a monochromator at intensities of  $\sim 1$  mWcm<sup>-2</sup>. Short circuit currents were recorded using a Keithley 237 source meter. The current–voltage characteristics of the device were measured under simulated 100 mW cm<sup>-2</sup> AM 1.5 illumination using an Abet Technology solar simulator. The spectral mismatch of the simulator was calibrated to a silicon reference cell.

*OFETs fabrication.* OFET devices were fabricated in a staggered bottom contacts top gate configuration. Low alkali 1737F Corning glasses were used as substrates; they were cleaned

in ultrasonic bath of Milli-Q water, acetone and isopropyl alcohol respectively and exposed to O<sub>2</sub> plasma at 100 W for 10 min. Bottom electrodes, 20 μm channel in width and 2 mm channel in length, were patterned by a lift-off photolithographic process and deposited by thermal evaporation of a 1.5 nm thick Cr, as adhesion layer, and 20 nm thick Au. After the lift-off process the substrates were cleaned in ultrasonic bath in isopropyl alcohol for 10 min and exposed to O<sub>2</sub> plasma at 100 W for 10 min. The semiconductor layer was deposited by spin coating at 1500 rpm for 30 s, starting from solutions at 5 mg/mL in oDCB filtered with PTFE, 0.20 μm pores. After the deposition of the semiconductor, the devices were annealed on a hot plate at 170 °C overnight under nitrogen atmosphere. Dielectric layers with thickness of 500 nm were obtained by spincoating the perfluorinated polymer CYTOP CTL-809M (Asahi Glass) at 5000 rpm for 90 s under nitrogen atmosphere. After the dielectric deposition, the devices were annealed under nitrogen, on a hot plate, at 80°C for 1 h. The 40 nm thick gate contact was obtained by thermal evaporation of Al through a shadow mask.

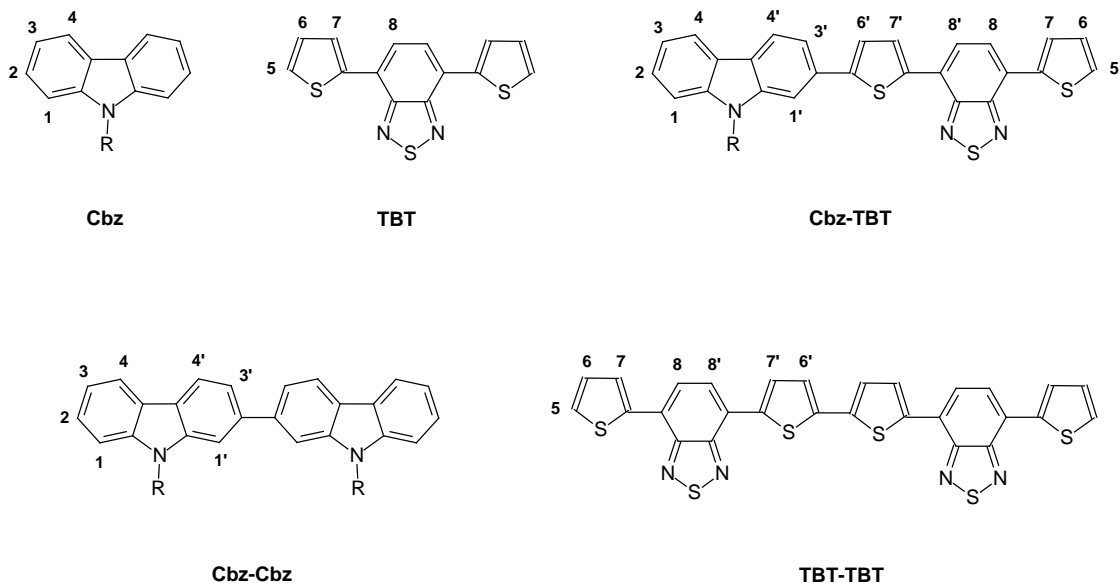
*OFET Characterization.* The electrical characteristics of transistors were measured in a nitrogen filled glovebox on a Wentworth Laboratories probe station with a semiconductor device analyser (Agilent B1500A). The saturation mobility values were calculated using the gradual-channel approximation.

**Table S1.** Overview of molecular weights of PCDTBT using relative PS calibration ( $M_{n,rel}$  and  $M_{w,rel}$ ) and universal calibration ( $M_{n,UC}$  and  $M_{w,UC}$ ) using viscosimetry

#	$M_{n,rel}$ [kDa]	$M_{w,rel}$ [kDa]	$M_{n,UC}$ [kDa]	$M_{w,UC}$ [kDa]	Mark- Houwink K ( $10^{-5}$ dL/g)	Mark- Houwink $\alpha$
<b>1</b>	8	32	4	20	225	0.55
<b>2</b>	10	33	4	14	583	0.50
<b>3</b>	12	33	7	22	265	0.52
<b>4</b>	7	35	3	18	765	0.45
<b>5</b>	10	30	4	15	254	0.54
<b>6</b>	12	41	9	28	40	0.70
<b>7</b>	23	72	6	32	1983	0.37
<b>8</b>	15	48	5	13	139	0.55
<b>9</b>	28	58	10	24	489	0.51
<b>10</b>	21	52	8	23	689	0.46
<b>11</b>	25	81	7	30	900	0.47

## Estimation of $^1\text{H}$ chemical shifts for PCDTBT substructures

### 1. Model compounds, experimental $^1\text{H}$ NMR chemical shifts and $^1\text{H}$ chemical shift effects



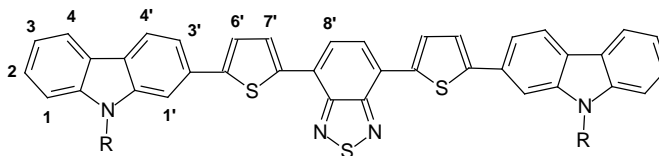
Position	$^1\text{H}$ NMR chemical shift (ppm) <sup>a)</sup>					$^1\text{H}$ chemical shift effect (ppm) <sup>b)</sup>	
	Cbz	TBT	Cbz-TBT	Cbz-Cbz	TBT-TBT	<i>TBT on Cbz</i>	<i>Cbz on TBT</i>
1	7.51	-	7.53	7.54	-	<b>+0.02</b>	
2	7.43	-	7.46	7.45	-	<b>+0.03</b>	
3	7.22	-	7.25	7.25	-	<b>+0.03</b>	
4	8.11	-	8.11	8.14	-	<b>0</b>	
5	-	7.49	7.50	-	7.51	-	<b>+0.01</b>
6	-	7.25	7.25	-	7.26	-	<b>0</b>
7	-	8.15	8.17	-	8.17	-	<b>+0.02</b>
8	-	7.91	7.93	-	7.93	-	<b>+0.02</b>
1'	-	-	7.83	7.82	-	<b>+0.32</b>	
3'	-	-	7.61	7.59	-	<b>+0.39</b>	
4'	-	-	8.13	8.18	-	<b>+0.02</b>	
6'	-	-	7.52	-	7.44	-	<b>+0.27</b>
7'	-	-	8.21	-	8.14	-	<b>+0.06</b>
8'	-	-	7.95	-	7.93	-	<b>+0.04</b>

<sup>a)</sup> Measured in  $\text{C}_2\text{D}_2\text{Cl}_4$  at  $120^\circ\text{C}$ .

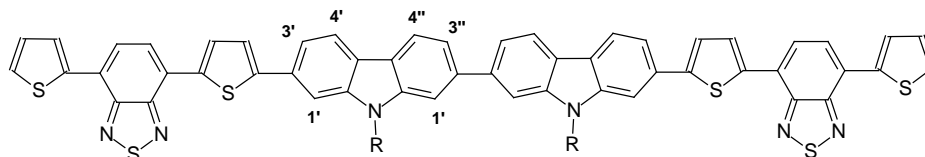
<sup>b)</sup> Calculated from the  $^1\text{H}$  chemical shift of the proton in Cbz-TBT minus the  $^1\text{H}$  chemical shift of the corresponding proton in Cbz and TBT, respectively.

2. Test compound Cbz-TBT-Cbz and model structures TBT-Cbz-Cbz-TBT and TBT-Cbz-Cbz-TBT for Cbz-Cbz and TBT-TBT homocouplings, resp., in PCBTBT and comparison of calculated and experimentally observed  $^1\text{H}$  chemical shifts

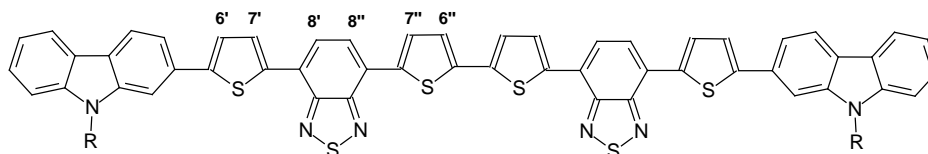
Cbz-TBT-Cbz



TBT-Cbz-Cbz-TBT



Cbz-TBT-TBT-Cbz



Position	$^1\text{H}$ NMR chemical shift (ppm) <sup>a)</sup>					
	Cbz-TBT-Cbz <sup>b)</sup>		TBT-Cbz-Cbz-TBT <sup>c)</sup>		Cbz-TBT-TBT-Cbz <sup>d)</sup>	
	Calc.	Exp.	Calc.	Exp.	Calc.	Exp.
1	7.53	7.54	-	-	-	-
2	7.46	7.46	-	-	-	-
3	7.25	7.26	-	-	-	-
4	8.11	8.12	-	-	-	-
1'	7.83	7.84	7.86	7.88	-	-
3'	7.61	7.62	7.64	7.66	-	-
4'	8.13	8.14	8.16	8.18	-	-
1''	-	-	7.84	7.87	-	-
3''	-	-	7.62	7.64	-	-
4''	-	-	8.18	8.22	-	-
6'	7.52	7.53	-	-	7.53	n. i.
7'	8.23	8.23	-	-	8.23	n. i.
8'	7.97	7.98	-	-	7.97	n. i.
6''	-	-	-	-	7.44	7.47
7''	-	-	-	-	8.16	8.18
8''	-	-	-	-	7.95	n. i.

<sup>a)</sup> Measured in  $\text{C}_2\text{D}_2\text{Cl}_4$  at  $120^\circ\text{C}$  and calculated for same conditions.

<sup>b)</sup> Values for positions 1 -4' from Cbz-TBT and the values of positions 6' – 8' were calculated from TBT chemical shifts and chemical shift effects of *Cbz on TBT*. Experimental values from authentic Cbz-TBT-Cbz sample.

<sup>c)</sup> Values of positions 1' – 4'' were calculated from Cbz-Cbz chemical shifts and chemical shift effects of *TBT on Cbz*. Experimental values from PCDTBT **6** (see **Figures SI-2 and SI-3**).

<sup>d)</sup> Values of positions 6' – 8'' were calculated from TBT-TBT chemical shifts and chemical shift effects of *Cbz on TBT*. Experimental values from PCDTBT **8** (see **Figures SI-4 and SI-5**). N. i. – not identified due to signal overlap.



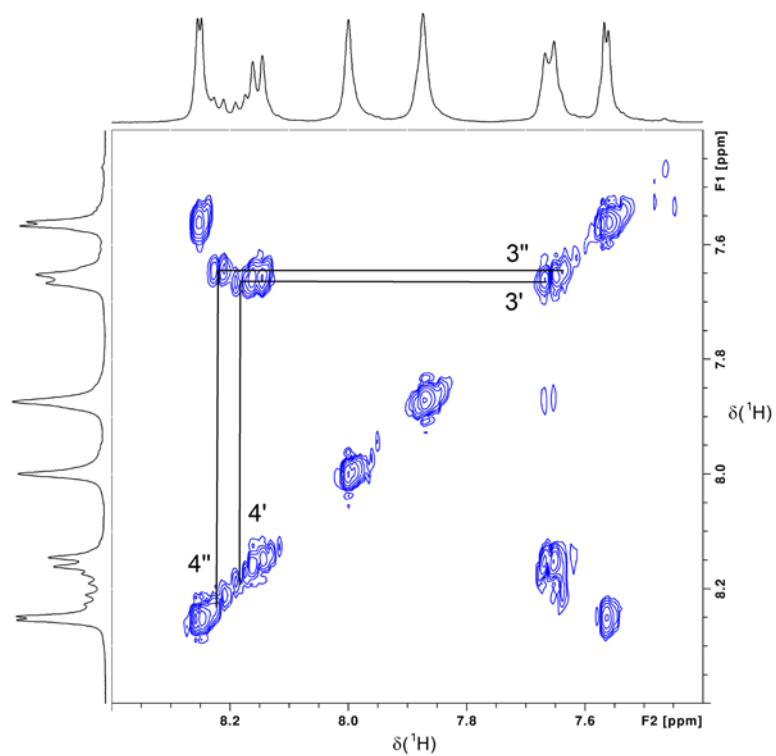


**Figure SI-2.** COSY spectrum (region) of PCDTBT **6** containing TBT-Cbz-Cbz-TBT substructures. The  $^3J_{\text{HH}}$  correlations  $\text{H}_{3'} - \text{H}_{4'}$  and  $\text{H}_{3''} - \text{H}_{4''}$  are marked. Solvent  $\text{C}_2\text{D}_2\text{Cl}_4$  at  $120^\circ\text{C}$ .

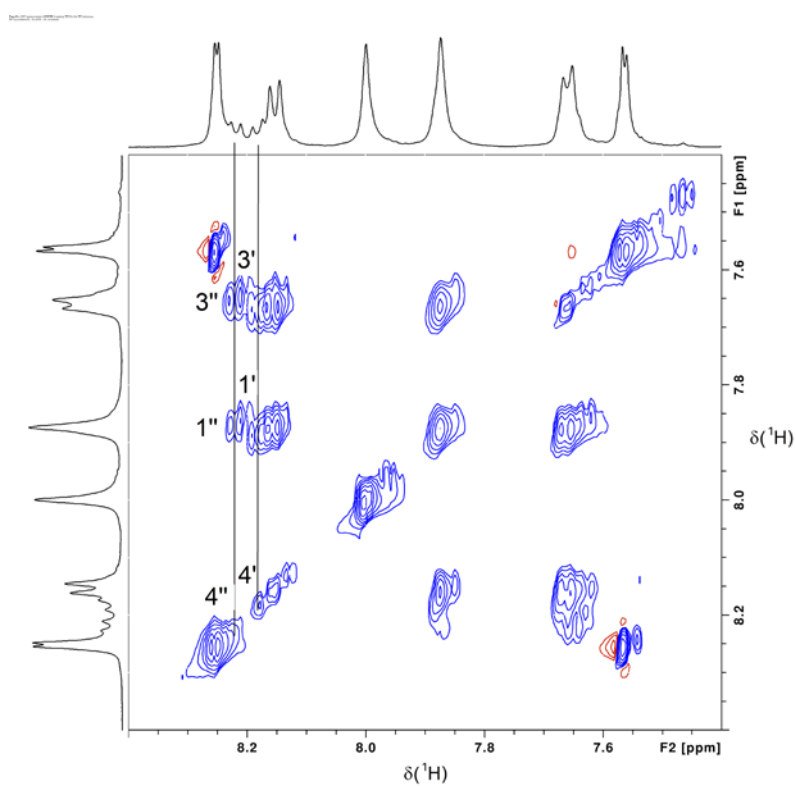


**Figure SI-3.** TOCSY spectrum (region) of PCDTBT **6** containing TBT-Cbz-Cbz-TBT substructures. The correlations additionally allow the assignment of  $\text{H}_{1'}$  and  $\text{H}_{1''}$ . Solvent  $\text{C}_2\text{D}_2\text{Cl}_4$  at  $120^\circ\text{C}$ .

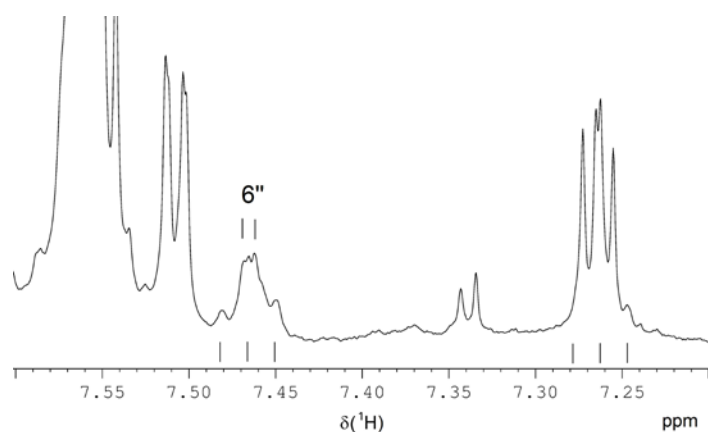


**Figure SI-4.** Region of the  $^1\text{H}$  NMR spectrum of PCDTBT **8** showing the doublet of  $\text{H}_{6''}$  ( $J = 3.2$  Hz) overlapped by the  $\text{H}_2$  triplet of the Cbz-H end group ( $J = 7.5$  Hz). The  $\text{H}_3$  triplet of the Cbz-H end group is overlapped by a signal of the TBT-H end group. Solvent  $\text{C}_2\text{D}_2\text{Cl}_4$  at  $120^\circ\text{C}$ .

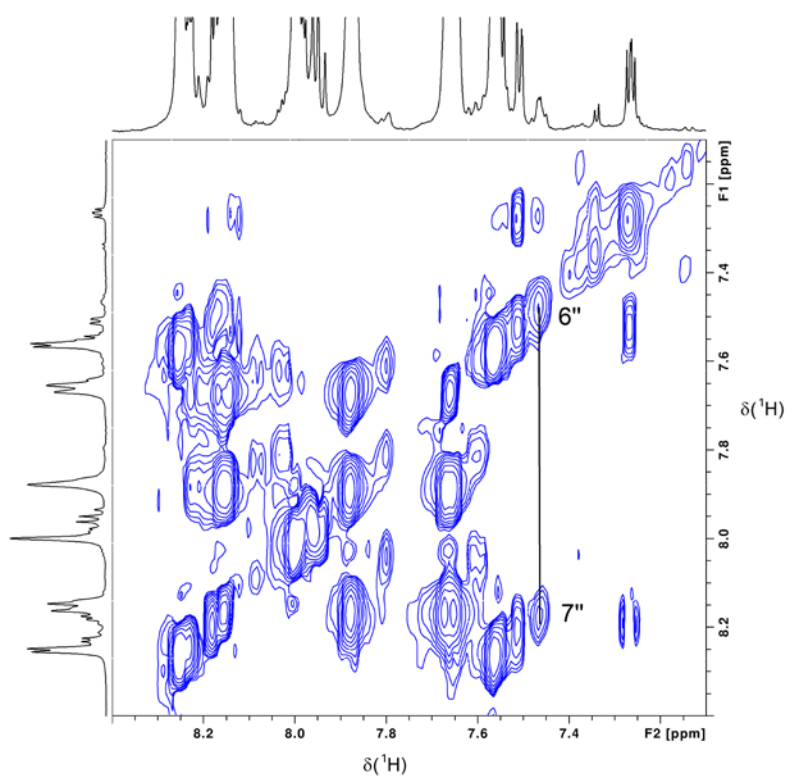


**Figure SI-5.** TOCSY spectrum (region) of PCDTBT **8** containing low content of Cbz-TBT-TBT-Cbz substructures. The correlation between  $\text{H}_{6''}$  and  $\text{H}_{7''}$  is marked. Solvent  $\text{C}_2\text{D}_2\text{Cl}_4$  at  $120^\circ\text{C}$ .

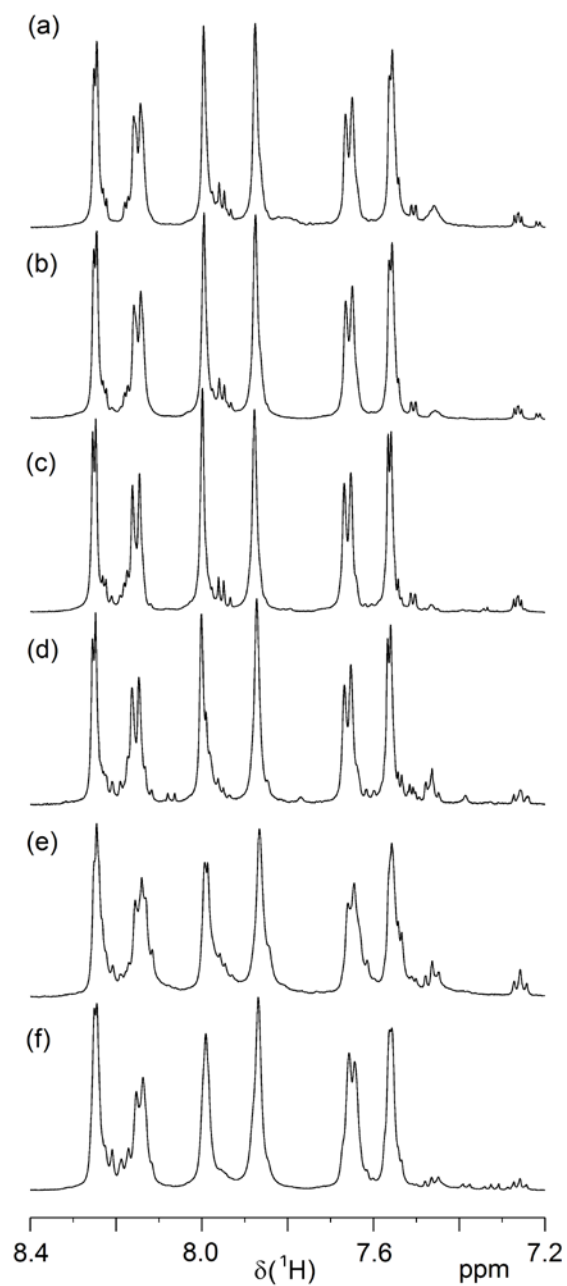


**Figure SI-6.** <sup>1</sup>H NMR spectra of PCDTBT **1** (a), **2** (b), **3** (c), **4** (d), **5** (e) and **10** (f). Solvent C<sub>2</sub>D<sub>2</sub>Cl<sub>4</sub> at 120°C.

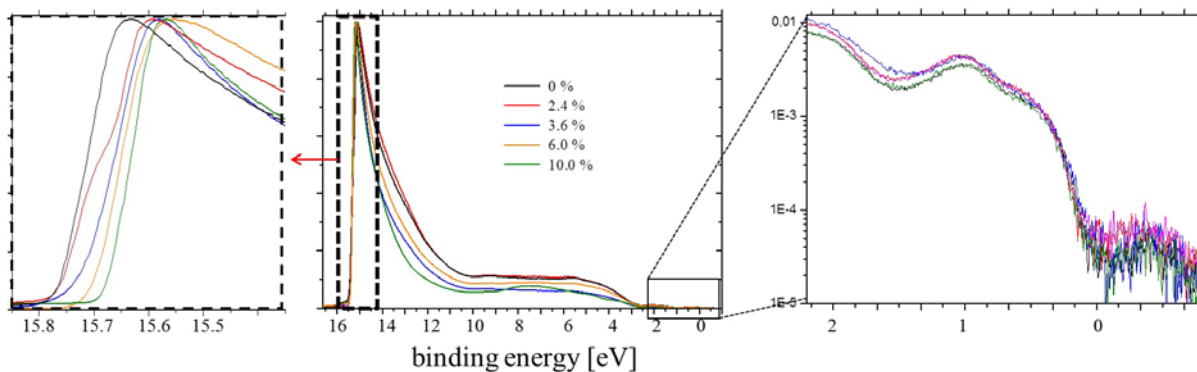


**Figure SI-7.** UPS spectra of PCDTBT **1** (0%), **2** (2.4%), **3** (3.6%), **4** (6%) and **6** (10%).

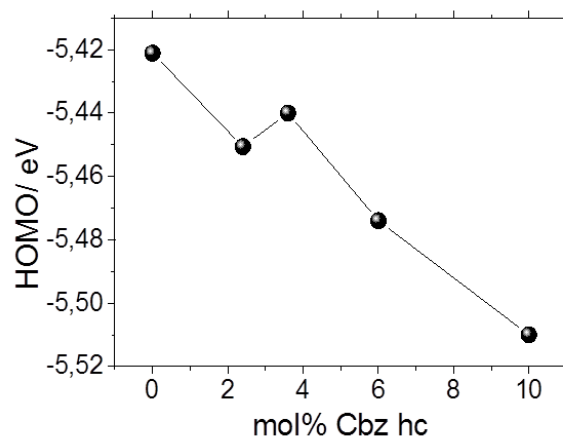


**Figure SI-8.** From UPS experiments extracted HOMO level positions of PCDTBT **1-4,6** plotted as a function of % Cbz hc. The vertical error bar of 0.15 eV is not shown for clarity.

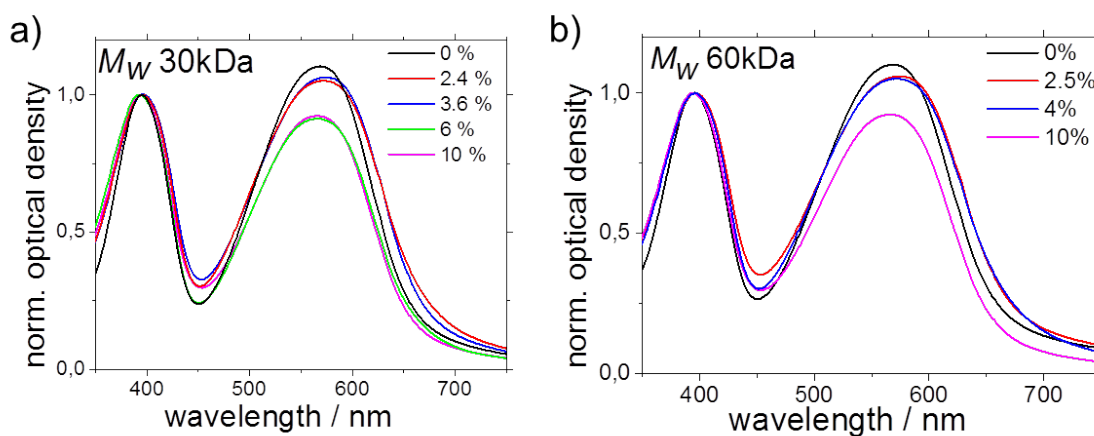


**Figure SI-9.** UV-vis absorption spectra of PCDTBT a) 30 kDa thin films; PCDTBT **1** (0%), **2** (2.4%), **3** (3.6%), **4** (6%) and **6** (10%). b) 60 kDa thin films; PCDTBT **7** (0%), **8** (2.5%), **9** (4%) and **10** (10%)

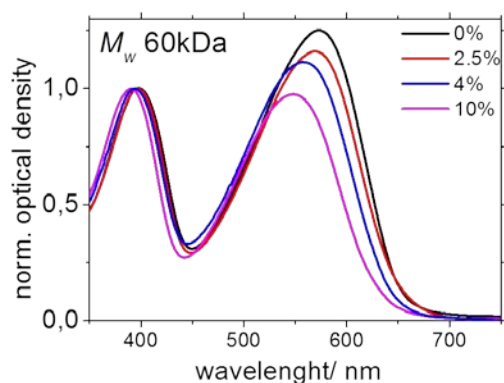


**Figure SI-10.** UV-vis absorption spectra in chlorobenzene; PCDTBT **7** (0%) **8** (2.5%), **9** (4%) and **10** (10%) ( $M_w \sim 60$ kDa).

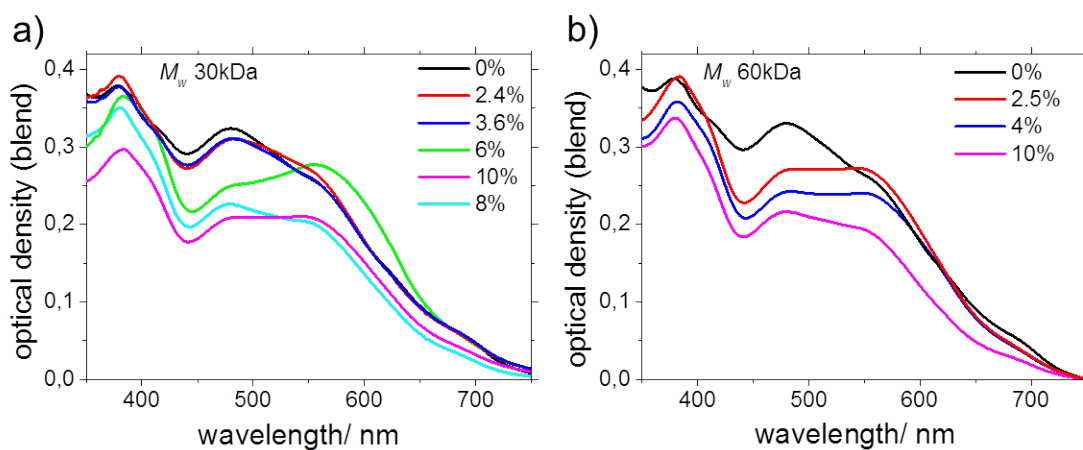


**Figure SI-11.** UV-vis absorption spectra of the PCDTBT:PC<sub>71</sub>BM (1:4) blend used for OPV; a) PCDTBT **1** (0%), **2** (2.4%), **3** (3.6%), **4** (6%) and **6** (10%). b) PCDTBT **7** (0%), **8** (2.5%), **9** (4%), **10** (10%).

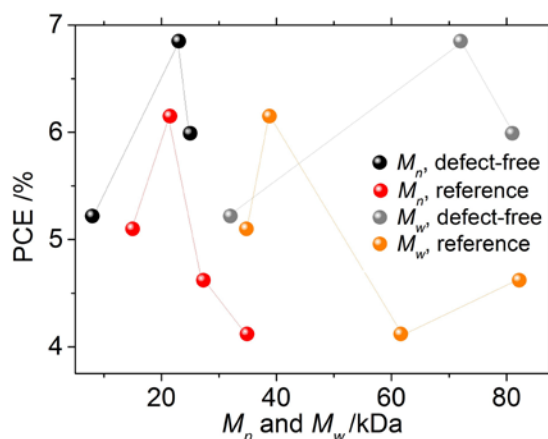


**Figure SI-12.** Correlation of  $M_n$ ,  $M_w$  and PCE. Reference data were taken from Kingsley *et al.*, defect-free samples are PCDTBT **1**, **7** and **11**.<sup>3</sup>

## DFT calculations

We report the Cartesian coordinates and absolute energies of the optimized PCDTBT oligomers (i.e. stable equilibrium minima) discussed in the main text.

Structures have been optimized using two DFT XC functionals, namely B3LYP-D3 and LC-BLYP-D3 ( $\mu = 0.21$ )

### LC-BLYP/6-311G\* ( $\mu = 0.21$ )

Alternating chain			
C	-35.294272	4.728696	1.906174
C	-33.906265	4.640756	1.780085
C	-33.146500	5.815968	1.571043
C	-33.769481	7.067379	1.488600
C	-35.152563	7.142133	1.615962
C	-35.903896	5.969538	1.823870
N	-31.799740	5.475054	1.478698
C	-31.684713	4.096819	1.624111
C	-32.971926	3.540169	1.815270
C	-33.105704	2.161578	1.987348
C	-31.975288	1.361199	1.967848
C	-30.691481	1.917471	1.787130
C	-30.543262	3.295893	1.614600
C	-29.518953	1.035280	1.789393
C	-29.339111	-0.132400	2.491994
C	-28.073677	-0.721509	2.274746
C	-27.274134	-0.013726	1.403348
S	-28.109802	1.415832	0.846601
C	-25.939180	-0.386772	0.948354
C	-25.423578	-1.651467	1.143972
C	-24.122127	-2.036975	0.739732
C	-23.237819	-1.188086	0.106692
C	-23.740336	0.128605	-0.146302
C	-25.067405	0.523217	0.267987
N	-23.074922	1.102318	-0.777048
S	-24.065470	2.400033	-0.832835
N	-25.367587	1.784519	-0.061343
C	-21.894282	-1.609325	-0.278031
C	-21.251263	-2.763498	0.114410
C	-19.971020	-2.923893	-0.460252
C	-19.620246	-1.890056	-1.295564
S	-20.875231	-0.689883	-1.359281
C	-18.371390	-1.719574	-2.047275
C	-17.182100	-2.228682	-1.519711
C	-16.007560	-2.080878	-2.256082
C	-16.003358	-1.416453	-3.506281
C	-17.196525	-0.903933	-4.017478
C	-18.367519	-1.059493	-3.294098
N	-14.714248	-2.493160	-1.952117
C	-13.874692	-2.105654	-2.991249
C	-14.639183	-1.434276	-3.977460
C	-14.012144	-0.948928	-5.126269
C	-12.648713	-1.130320	-5.285021
C	-11.886936	-1.806873	-4.309438
C	-12.501860	-2.299389	-3.155811
C	-10.446774	-1.991846	-4.520141
C	-9.776134	-2.144407	-5.710196
C	-8.384876	-2.324565	-5.543796
C	-7.976549	-2.309143	-4.227510
S	-9.349925	-2.071109	-3.174584
C	-6.607040	-2.425725	-3.737837
C	-5.515305	-2.300989	-4.572024
C	-4.175578	-2.434179	-4.132000
C	-3.826363	-2.702343	-2.824599
C	-4.926406	-2.810253	-1.914101
C	-6.293279	-2.674474	-2.362834
N	-4.823714	-3.026369	-0.598175
S	-6.342524	-3.049374	0.002465
N	-7.185680	-2.792109	-1.373299
C	-2.436787	-2.859514	-2.407885
S	-1.928432	-2.804461	-0.737979
C	-0.258714	-2.999841	-1.175711
C	-0.117320	-3.108286	-2.538968
C	-1.345427	-3.029686	-3.232374
C	0.790978	-3.043125	-0.151152
C	0.531493	-3.591296	1.122676
C	1.517434	-3.640689	2.094302
C	2.789817	-3.146610	1.803629
C	3.051324	-2.600010	0.524100
C	2.058194	-2.537752	-0.452465
C	4.016401	-3.037797	2.556403
C	4.968814	-2.430202	1.701072
N	4.372522	-2.168129	0.471833
C	6.267988	-2.171572	2.142452
C	6.620497	-2.535021	3.444476
C	5.673325	-3.149829	4.289847
C	4.381968	-3.395190	3.855326
C	7.973746	-2.273789	3.947776
C	8.360104	-2.005272	5.239048
C	9.751324	-1.800508	5.370606
C	10.444192	-1.907770	4.183855
S	9.346160	-2.300488	2.881568
C	11.878203	-1.716919	3.990754
C	12.695868	-1.219903	4.984920
C	14.093493	-1.048128	4.836803
C	14.779080	-1.337549	3.674916
C	13.970687	-1.851009	2.610430
C	12.546154	-2.037978	2.765588
N	14.418514	-2.205491	1.401026
S	13.128127	-2.726429	0.545901
N	<b>11.957528</b>	<b>-2.524943</b>	<b>1.667596</b>
C	<b>16.217167</b>	<b>-1.124682</b>	<b>3.544183</b>
C	<b>17.036977</b>	<b>-0.470316</b>	<b>4.438577</b>
C	<b>18.397195</b>	<b>-0.458321</b>	<b>4.059046</b>
C	<b>18.631224</b>	<b>-1.101139</b>	<b>2.866664</b>
S	<b>17.152645</b>	<b>-1.713493</b>	<b>2.190486</b>
C	19.909874	-1.271523	2.166746
C	20.888997	-0.281989	2.286942
C	22.110388	-0.462894	1.635278
C	22.353262	-1.618800	0.851276
C	21.362917	-2.594611	0.732598
C	20.155494	-2.421588	1.388496
N	23.233497	0.357318	1.592689
C	24.193513	-0.254351	0.793520
C	23.686695	-1.485792	0.314979
C	25.477925	0.177067	0.464299
C	26.262320	-0.628122	-0.365059
C	25.753036	-1.851355	-0.850706
C	24.481199	-2.281875	-0.512107
C	27.621627	-0.217391	-0.734172
C	28.708013	-1.018770	-0.992664
C	29.877732	-0.286947	-1.296344
C	29.698239	1.079238	-1.276056
S	28.044615	1.463135	-0.865807
C	30.699546	2.094246	-1.587012
C	31.888090	1.784293	-2.214626
C	32.892889	2.740390	-2.503252
C	32.784824	4.078173	-2.185324
C	31.551886	4.454315	-1.561527
C	30.526535	3.479286	-1.267093
N	31.212903	5.698100	-1.204965
S	29.716266	5.618100	-0.555852
N	29.441113	4.013339	-0.695993
C	33.852220	5.032827	-2.468294
S	33.616612	6.766808	-2.458800
C	35.259347	7.055847	-2.935087
C	35.945716	5.879378	-3.072033
C	35.152206	4.735847	-2.807150
C	35.770672	8.448163	-3.119734
C	23.401374	1.652707	2.250844
C	22.427204	2.692418	1.701239
C	5.000783	-1.547067	-0.694121
C	6.153909	-2.393470	-1.229091
C	-14.332131	-3.211437	-0.736394
C	-13.358837	-2.398782	0.114701
C	-30.676012	6.385066	1.261664
C	-30.516353	7.366130	2.421198
C	-35.855895	8.470868	1.534824
C	-13.821638	-4.616004	-1.050805
C	-30.767453	7.076061	-0.097171
C	5.401411	-0.100657	-0.412411
C	23.341606	1.521919	3.771068
H	37.000543	5.839548	-3.348036
H	35.536113	3.715989	-2.846244
H	33.787127	2.391710	-3.023943
H	32.066004	0.754019	-2.529740
H	30.842599	-0.754168	-1.495807
H	28.671050	-2.106118	-0.921043
H	26.369495	-2.447983	-1.526117
H	25.890645	1.108223	0.858843
H	21.539816	-3.492050	0.134388
H	19.386323	-3.194467	1.325288
H	20.667222	0.619093	2.858952
H	23.567789	2.488445	4.244058
H	22.348136	1.203799	4.116094
H	24.073862	0.783772	4.126139
H	22.638038	3.678840	2.139013
H	22.521291	2.772549	0.609527
H	21.383158	2.439118	1.931404
H	36.828091	8.422027	-3.416414
H	35.217642	8.990234	-3.901314
H	35.697649	9.039517	-2.194764









C 10.523838 0.191251 -4.004380  
S 9.382334 1.053857 -2.985964  
C 11.961388 0.193620 -3.779869  
C 12.859472 -0.153956 -4.777525  
C 14.258583 -0.191092 -4.597308  
C 14.891366 0.117880 -3.402951  
C 14.008652 0.516626 -2.343518  
C 12.565836 0.553347 -2.528226  
N 14.387612 0.888975 -1.120800  
S 13.030592 1.257388 -0.281573  
N 11.910693 0.952105 -1.437526  
C 16.337436 0.042461 -3.254974  
C 17.221378 -0.606000 -4.096788  
C 18.575706 -0.454975 -3.735171  
C 18.762029 0.311768 -2.605520  
S 17.224175 0.832581 -1.961048  
C 20.025100 0.656056 -1.948009  
C 21.091783 -0.252117 -1.998295  
C 22.301090 0.088721 -1.394451  
C 22.454973 1.331477 -0.721811  
C 21.382637 2.225328 -0.669572  
C 20.184497 1.891059 -1.277830  
N 23.494637 -0.624554 -1.304101  
C 24.410023 0.142130 -0.587202  
C 23.798580 1.365977 -0.210620  
C 25.732941 -0.136572 -0.251997  
C 26.462385 0.811973 0.477979  
C 25.846395 2.027948 0.859043  
C 24.533811 2.305548 0.517529  
C 27.857252 0.564139 0.848176  
C 28.872025 1.484150 0.996859  
C 30.111170 0.905331 1.340338  
C 30.075693 -0.470231 1.468383  
S 28.451448 -1.052375 1.143059  
C 31.177216 -1.337479 1.859654  
C 32.312717 -0.843112 2.481758  
C 33.418487 -1.641527 2.847794  
C 33.490972 -3.006917 2.624422  
C 32.323822 -3.578459 2.015262  
C 31.183530 -2.756241 1.638692  
S 32.148593 -4.871270 1.739415  
N 30.664094 -5.027641 1.066233  
C 30.190841 -3.459573 1.093194  
C 34.669667 -3.783038 2.986789  
S 34.648797 -5.524180 3.241396  
C 36.330736 -5.544617 3.691351  
C 36.867600 -4.286704 3.625274  
C 35.936291 -3.295759 3.228364  
C 37.016668 -6.825104 4.056293  
C 23.771140 -1.957535 -1.854011  
C 22.908874 -3.037001 -1.188920  
C 4.931625 1.740671 0.499131  
C 6.058329 2.767692 0.665447  
C -14.504890 3.262067 -0.279257  
C -15.148300 4.527288 -0.859031  
C -30.888346 -6.569764 0.497346  
C -30.599029 -7.853720 -0.289109  
C -36.036876 -8.789641 0.428399  
C -14.692497 2.023878 -1.164012  
C -31.101814 -6.809617 1.996771  
C 5.354339 0.311894 0.860866  
C 23.687486 -1.968498 -3.384777  
H 37.908797 -4.080334 3.845241  
H 36.199310 -2.253151 3.100119  
H 34.238596 -1.148835 3.357386  
H 32.357765 0.210031 2.734267  
H 31.020115 1.482437 1.455334  
H 28.735321 2.542822 0.814864  
H 26.407607 2.738211 1.455129  
H 26.213844 -1.054095 -0.568773  
H 21.490055 3.179693 -0.164045  
H 19.362240 2.597641 -1.264290  
H 20.946678 -1.209941 -2.477112  
H 24.003985 -2.941078 -3.770333  
H 22.674087 -1.781355 -3.742465  
H 24.339738 -1.202020 -3.808637  
H 23.214204 -4.027371 -1.536637  
H 23.025572 -3.003610 -0.103665  
H 21.848676 -2.915895 -1.415276  
H 38.062842 -6.631877 4.302877  
H 36.552289 -7.304431 4.923613  
H 36.995071 -7.547523 3.234483  
H 24.076991 3.241720 0.822538  
H 19.397666 -0.873471 -4.303050  
H 16.901017 -1.184660 -4.954133  
H 14.861009 -0.449638 -5.460417  
H 12.482353 -0.385260 -5.767004  
H 10.343158 -1.043663 -5.778865  
H 7.775410 -0.644414 -5.751449  
H 6.047794 1.063414 -5.728427  
H 6.977182 0.995932 -1.531203  
H 1.316412 2.422508 -4.057553  
H -0.490656 3.021690 -2.493920  
H 2.126491 2.434008 0.871141  
H 5.701416 0.274618 1.896782  
H 4.511402 -0.374493 0.755986  
H 6.163700 -0.051102 0.225836  
H 6.407500 2.773915 1.701235  
H 6.915546 2.549182 0.027417  
H 5.701991 3.769711 0.416896  
H 3.714579 1.703152 -5.242199  
H 0.664189 4.119003 1.835341

H -1.623442 4.453420 3.026038  
H -3.574910 3.676643 3.872005  
H -5.850431 3.735597 4.636532  
H -7.878980 4.501050 5.180752  
H -10.437523 4.312775 5.590055  
H -12.328048 2.790843 5.635040  
H -12.143322 3.481414 1.391783  
H -17.398337 2.104013 4.694921  
H -19.509489 1.952270 3.431064  
H -17.441514 2.730730 -0.256119  
H -14.266756 2.202753 -2.154801  
H -14.187792 1.160886 -0.724621  
H -15.744552 1.766142 -1.293679  
H -14.718323 4.749121 -1.839164  
H -16.226699 4.421252 -0.984540  
H -14.969094 5.382527 -0.204072  
H -14.765264 2.428316 5.510840  
H -19.589846 3.741085 -0.804070  
H -21.955356 3.151598 -1.704966  
H -23.531133 1.742805 -2.439950  
H -25.709250 0.888047 -2.964243  
H -27.902388 0.714051 -3.203810  
H -30.157053 -0.552017 -3.432144  
H -32.222402 -1.071985 -2.316333  
H -29.755928 -4.085264 -0.485678  
H -36.010003 -4.547695 -1.531502  
H -37.117635 -6.634179 -0.798901  
H -33.405450 -8.173886 0.699669  
H -30.215670 -7.280569 2.430291  
H -31.275091 -5.863437 2.513773  
H -31.955420 -7.459788 2.192757  
H -29.709961 -8.347372 0.111978  
H -31.427119 -8.562131 -0.238339  
H -30.418946 -7.624061 -1.341508  
H -34.215046 -2.507600 -2.089934  
H -36.504266 -9.293353 -0.423822  
H -35.355991 -9.501310 0.900558  
H -36.834118 -8.568025 1.145121  
H -30.011289 -5.928319 0.399373  
H -13.432396 3.450472 -0.213875  
H 4.135000 2.025922 1.188029  
H 24.808257 -2.167295 -1.588315

E = -9982.92799290 a.u.

Cbz-Cbz

S 34.306906 -3.065143 -3.123748  
C 33.500603 -4.590259 -2.776400  
C 34.367923 -5.635583 -3.011120  
C 35.643729 -5.230977 -3.475465  
C 35.773290 -3.873629 -3.601111  
C 32.108979 -4.688542 -2.356108  
C 31.380789 -5.857087 -2.508791  
C 30.041112 -6.008103 -2.088054  
C 29.307317 -5.003538 -1.477698  
C 30.003487 -3.756922 -1.327022  
C 31.384479 -3.602586 -1.759291  
N 29.492860 -2.642265 -0.802888  
S 30.664585 -1.498544 -0.859431  
N 31.864470 -2.377130 -1.544901  
C 27.938054 -5.216429 -1.032332  
C 27.321691 -6.432535 -0.808542  
C 25.964072 -6.330670 -0.440686  
C 25.508535 -5.032249 -0.370110  
S 26.791320 -3.914018 -0.767625  
C 24.169770 -4.566335 -0.002853  
C 23.046838 -5.375430 -0.299435  
C 21.765769 -4.979213 0.044408  
C 21.573958 -3.753318 0.687787  
C 22.696003 -2.934250 0.976995  
C 23.987290 -3.335016 0.641732  
C 20.414894 -3.052588 1.170594  
C 20.876160 -1.834260 1.739014  
N 22.262763 -1.774562 1.614926  
C 19.980972 -0.916603 2.286406  
C 18.611318 -1.215568 2.283829  
C 18.159044 -2.430821 1.719359  
C 19.047318 -3.337754 1.166680  
C 17.669543 -0.261866 2.874800  
C 17.884140 0.605245 3.924119  
C 16.764858 1.404972 4.232418  
C 15.664502 1.169401 3.429380  
S 16.054419 -0.062669 2.239524  
C 14.356565 1.799129 3.536788  
C 13.973672 2.512801 4.662417  
C 12.726392 3.159218 4.796968  
C 11.745161 3.154788 3.817142  
C 12.076968 2.402268 2.640360  
C 13.362474 1.734689 2.502951  
N 11.283432 2.227776 1.583165  
S 12.097913 1.294266 0.511629  
N 13.490049 1.081977 1.347578  
C 10.485527 3.863116 3.985066  
C 10.208838 4.854969 4.907068  
C 8.879034 5.322711 4.868803  
C 8.104843 4.702610 3.912340  
S 9.045045 3.513206 3.043916  
C 6.700043 4.952041 3.583260



N	-34.242383	2.096997	-0.891783	C	35.230374	5.284493	1.723010
C	-35.524645	2.031971	-1.432870	C	36.618793	5.283181	1.607794
C	-35.701303	0.774901	-2.062111	C	37.243502	4.441757	0.664843
C	-36.550235	2.982061	-1.421246	C	36.503494	3.607411	-0.157552
C	-37.760815	2.679150	-2.040735	C	37.463732	6.172490	2.487854
C	-37.933007	1.426992	-2.666554	C	32.065135	4.933750	1.613638
C	-36.920065	0.481149	-2.680720	C	32.031621	6.443836	1.349144
C	-33.693987	3.255046	-0.175914	C	14.573788	-1.796084	-1.917434
C	-33.390251	2.925617	1.290555	C	14.960881	-2.308316	-3.309673
C	-32.502155	3.871428	-0.918665	C	-14.599609	-1.058222	-0.058695
C	-18.661780	0.570788	1.051588	C	-14.032923	-0.964258	-1.480318
C	-17.466605	-0.050174	0.661996	C	-13.687953	-1.820982	0.910165
C	-16.270178	0.651821	0.786133	C	14.873035	-0.306251	-1.712374
C	-16.247203	1.981854	1.282339	C	32.180587	4.579481	3.100971
C	-17.444462	2.594654	1.660816	H	-0.314611	-3.400464	1.544445
C	-18.634210	1.894960	1.549131	H	2.008202	-4.510530	1.846788
N	-14.971480	0.261233	0.467660	H	4.119058	-4.670535	2.500722
C	-14.113016	1.319850	0.754178	H	6.426593	-5.301150	2.639325
C	-14.873795	2.407091	1.261644	H	8.369967	-6.282957	2.172581
C	-12.731771	1.423762	0.598880	H	10.955449	-6.521142	2.169551
C	-12.091917	2.616482	0.963068	H	13.031263	-5.549831	2.928139
C	-12.853677	3.692361	1.477059	H	12.363831	-3.034256	-0.499525
C	-14.226822	3.592822	1.620823	H	18.038980	-4.636293	1.874182
C	-10.643248	2.762334	0.810616	H	20.027600	-3.740440	0.728250
C	-9.925647	3.912899	0.564899	H	17.547581	-1.577057	-2.038485
C	-8.535562	3.701098	0.473747	H	14.419188	-1.750201	-4.077699
C	-8.150208	2.384244	0.647461	H	16.027943	-2.197059	-3.506840
S	-9.567335	1.393689	0.963652	H	14.709336	-3.366072	-3.412035
C	-6.799201	1.851536	0.564694	H	14.343594	0.289228	-2.460712
C	-5.742135	2.597704	0.063263	H	14.544518	0.016734	-0.722252
C	-4.414088	2.130204	-0.009033	H	15.937549	-0.084211	-1.800128
C	-4.018586	0.860514	0.387005	H	15.473098	-5.312810	2.677399
C	-5.074471	0.042946	0.913717	H	19.431909	-1.915710	-3.480684
C	-6.442728	0.530480	1.000119	H	21.769885	-0.977450	-4.105414
N	-4.935122	-1.202821	1.366880	H	23.971083	-0.955757	-4.205065
S	-6.412746	-1.710964	1.858555	H	26.242875	-0.224775	-4.371768
N	-7.283617	-0.367484	1.513713	H	28.404528	-0.052204	-4.507296
C	-2.644160	0.406675	0.256738	H	30.813227	0.864292	-4.224207
S	-2.005419	-0.997468	1.098167	H	32.841884	0.633344	-2.951013
C	-0.405524	-0.744503	0.435504	H	30.679171	3.162590	-0.223057
C	-0.392050	0.363861	-0.389222	H	36.999524	2.965114	-0.878717
C	-1.640987	1.002955	-0.487094	H	34.759454	5.933397	2.449867
C	0.679029	-1.639565	0.754824	H	31.183881	6.897123	1.869674
C	0.618417	-2.907552	1.299989	H	32.939461	6.941859	1.692486
C	1.880606	-3.506336	1.463234	H	31.924140	6.641708	0.280514
C	2.941159	-2.718109	1.051751	H	31.340130	5.006730	3.654270
S	2.339183	-1.185318	0.438373	H	32.165820	3.496067	3.237348
C	4.354174	-3.048510	1.130654	H	33.101510	4.960281	3.544724
C	4.821698	-4.104065	1.900720	H	34.990018	1.566631	-2.177093
C	6.179370	-4.475766	1.981857	H	-19.328544	-2.211534	1.349901
C	7.200275	-3.829954	1.299205	H	-21.806754	-2.936051	1.040251
C	6.776159	-2.705565	0.513337	H	-23.733147	-3.035881	-0.126510
C	5.375356	-2.320481	0.431551	H	-26.087122	-3.281480	-0.535984
N	7.576984	-1.910966	-0.197153	H	-28.271974	-3.611228	-0.101007
S	6.633997	-0.772356	-0.902083	H	-30.802173	-3.406092	-0.660885
N	5.172849	-1.249786	-0.336043	H	-32.401461	-2.602162	-2.294884
C	8.583023	-4.271850	1.384631	H	-31.640208	1.101275	-0.248792
C	9.036219	-5.487182	1.864030	H	-37.070448	-0.477586	-3.167425
C	10.439416	-5.618362	1.867593	H	-38.882175	1.205207	-3.145612
C	11.097652	-4.507319	1.385792	H	-36.421649	3.946038	-0.940993
S	9.951627	-3.272522	0.922832	H	-33.090557	3.831429	1.824246
C	12.539763	-4.312732	1.225779	H	-34.275029	2.514045	1.781000
C	13.433228	-4.957374	2.114370	H	-32.583245	2.198698	1.390119
C	14.803958	-4.813213	1.984058	H	-32.189539	4.794446	-0.423379
C	15.318017	-4.009838	0.962254	H	-31.641831	3.201594	-0.947654
C	14.424980	-3.352375	0.076644	H	-32.776250	4.109946	-1.948597
C	13.045915	-3.503340	0.199120	H	-34.693220	-1.872077	-2.846913
C	16.648146	-3.653904	0.547611	H	0.489044	0.684847	-0.931292
C	16.513932	-2.794965	-0.576782	H	-1.810353	1.866920	-1.116934
N	15.159302	-2.618926	-0.851744	H	-3.669625	2.818412	-0.392147
C	17.922742	-3.977435	1.019596	H	-5.930489	3.599918	-0.303317
C	19.038551	-3.462277	0.381998	H	-7.831789	4.502791	0.289147
C	18.911690	-2.606530	-0.736930	H	-10.393615	4.879486	0.426297
C	17.636848	-2.265477	-1.210357	H	-12.345439	4.596753	1.790901
C	20.093844	-2.082269	-1.424700	H	-12.151048	0.615465	0.177350
C	20.226350	-1.766888	-2.759672	H	-17.443025	3.608683	2.047680
C	21.503083	-1.275982	-3.099484	H	-19.559101	2.358958	1.872758
C	22.382237	-1.205211	-2.034967	H	-17.498602	-1.047514	0.241003
S	21.576259	-1.735774	-0.566996	H	-13.870670	-1.966245	-1.886057
C	23.779613	-0.800878	-2.084014	H	-14.729728	-0.437157	-2.135523
C	24.473701	-0.697800	-3.280108	H	-13.079390	-0.435270	-1.509697
C	25.819373	-0.286465	-3.376224	H	-13.518814	-2.836553	0.542860
C	26.610669	0.035536	-2.283183	H	-12.714535	-1.342765	1.025622
C	25.941545	-0.060331	-1.016033	H	-14.148992	-1.885295	1.898149
C	24.548796	-0.470967	-0.918249	H	-14.795318	4.426310	2.021059
N	26.490666	0.203091	0.169800	H	38.326685	4.452134	0.586226
S	25.340194	-0.049545	1.307861	H	38.097608	6.835618	1.890691
N	24.101060	-0.501540	0.337149	H	36.851899	6.798766	3.140895
C	28.006396	0.421664	-2.424982	H	38.130207	5.581904	3.124897
C	28.775964	0.345913	-3.571545	H	-34.493078	3.997912	-0.179975
C	30.091237	0.827599	-3.418005	H	-15.536085	-1.614574	-0.121980
C	30.365339	1.285941	-2.147797	H	13.494935	-1.923655	-1.817991
S	28.970066	1.089091	-1.114356	H	31.116922	4.525650	1.260599
C	31.621461	1.843106	-1.641402	C	-38.893567	3.677141	-2.047624
C	32.849834	1.406198	-2.191044	H	-38.619339	4.608063	-1.546428
C	34.057546	1.918310	-1.746838	H	-39.196013	3.927172	-3.069541
C	34.067226	2.878368	-0.731781	H	-39.777970	3.276606	-1.541665
C	32.837931	3.312285	-0.171690				
C	31.620938	2.806515	-0.623090				
C	35.109818	3.600462	-0.050508				
C	34.475342	4.445656	0.895511				
N	33.095918	4.263758	0.812057				

E = -9982.92886269 a.u.

## Frontier molecular orbital energies (LC-BLYP/6-311G\*)

	HOMO / eV	LUMO / eV
Alternating	-6.52	-1.35
Cbz-Cbz hc	-6.54	-1.30
TBT-TBT hc	-6.50	-1.49

## Hole reorganization energy (LC-BLYP/6-311G\*)

	$\lambda$ / eV
Alternating	0.54
Cbz-Cbz hc	0.51
TBT-TBT hc	0.52

---

<sup>1</sup> F. Lombeck, R. Matsidik, H. Komber, M. Sommer, *Macromol. Rapid Commun.* **2015**, *36*, 231.

<sup>2</sup> N. Blouin, A. Michaud, M. Leclerc, *Adv. Mater.* **2007**, *19*, 2295.

<sup>3</sup> J. W. Kingsley, P. P. Marchisio, H. Yi, A. Iraqi, C. J. Kinane, S. Langridge, R. L. Thompson, A. J. Cadby, A. J. Pearson, D. G. Lidzey, R. A. L. Jones, A. J. Parnell, *Sci. Rep.* **2014**, *4*, DOI 10.1038/srep05286.

<sup>4</sup> J.C. DeMello, H.F. Wittmann, R.H. Friend, *Adv. Mater.* **1997**, *9*, 230–232.